Modular Pulse Synthesizer for Transcranial Magnetic Stimulation with Fully Adjustable Pulse Shape and Sequence

Z. Li[1], **J. Zhang**[1], **A. V. Peterchev**[1,2,3,4,5], **S. M. Goetz**[1,2,3,5,6]

[1]Department of Electrical and Computer Engineering, Duke University, Durham, NC 27708, United States of America.

[2]Department of Psychiatry and Behavioral Sciences, Duke University, Durham, NC 27710, United States of America.

[3]Department of Neurosurgery, Duke University, Durham, NC 27710, United States of America.

[4]Department of Biomedical Engineering, Duke University, Durham, NC 27708, United States of America.

[5]Duke Institute for Brain Sciences, Duke University, Durham, NC 27708, United States of America.

[6]Department of Engineering, University of Cambridge, Cambridge CB2 1PZ, United Kingdom.

Abstract

The temporal shape of a pulse in transcranial magnetic stimulation (TMS) influences which neuron populations are activated preferentially as well as the strength and even direction of neuromodulation effects. Furthermore, various pulse shapes differ in their efficiency, coil heating, sensory perception, and clicking sound. However, the available TMS pulse shape repertoire is still very limited to a few biphasic, monophasic, and polyphasic pulses with sinusoidal or near-rectangular shapes. Monophasic pulses, though found to be more selective and stronger in neuromodulation, are generated inefficiently and therefore only available in simple low-frequency repetitive protocols. Despite a strong interest to exploit the temporal effects of TMS pulse shapes and pulse sequences, waveform control is relatively inflexible and only possible parametrically within certain limits. Previously proposed approaches for flexible pulse shape control, such as through power electronic inverters, have significant limitations: The semiconductor switches can fail under the immense electrical stress associated with free pulse shaping, and most conventional power inverter topologies are incapable of generating smooth electric fields or existing pulse shapes.

Leveraging intensive preliminary work on modular power electronics, we present a modular pulse synthesizer (MPS) technology that can, for the first time, flexibly generate high-power TMS pulses (one-side peak ~ 4,000 V, ~ 8,000 A) with user-defined electric field shape as well as rapid sequences of pulses with high output quality. The circuit topology breaks the problem of simultaneous high power and switching speed into smaller, manageable portions, distributed across several identical modules. In consequence, MPS TMS can use semiconductor devices with voltage and current ratings lower than the overall pulse voltage and distribute the overall switching

of several hundred kilohertz among multiple transistors. MPS TMS can synthesize practically any pulse shape, including conventional ones, with fine quantization of the induced electric field (17% granularity without modulation and ~300 kHz bandwidth). Moreover, the technology allows optional symmetric differential coil driving so that the average electric potential of the coil, in contrast to conventional TMS devices, stays constant to prevent capacitive artifacts in sensitive recording amplifiers, such as electroencephalography (EEG).

MPS TMS can enable the optimization of stimulation paradigms for more sophisticated probing of brain function as well as stronger and more selective neuromodulation, further expanding the parameter space available to users.

Keywords

Transcranial magnetic stimulation; flexible pulse shape synthesis; arbitrary waveform generation; pulse sequence control; temporal control flexibility; electric field quantization; activation selectivity

Introduction

Magnetic stimulation is a technique to noninvasively stimulate neurons in the brain of conscious humans, and also in the spine or the peripheral nervous system [1–7]. Transcranial magnetic stimulation (TMS) causes neurons to fire action potentials in response to strong brief current pulses that generate magnetic fields reaching across the skull and inducing electric fields in a relatively focal target location [8, 9]. In addition to such *writing* of artificial signals into the brain, certain rhythms and patterns can further modulate neuronal circuits, i.e., influence how circuits process endogenous signals they receive [10]. TMS has become a key tool in experimental brain research and is widely used in medical diagnosis and treatment [11–14]. It is, for example, FDA-cleared for the treatment of depression, obsessive compulsive disorder, smoking addiction, and migraine as well as for cortical mapping [15–24]. TMS is also under investigation for many other disorders [1, 11, 25–27].

The spatial focality is largely determined by the TMS coil design and can be on the order of 0.5–1 cm^3, corresponding to approximately a million neurons [28–30]. Although TMS is typically called focal, it simultaneously activates neurons of different types and functions across an entire gyral crown—including inhibitory and excitatory neuron populations as well as projections from other circuits [31–37]. Thus, a pulse can even simultaneously activate neurons that counteract each other. Presumably as a consequence of this limited selectivity, the neuromodulatory and therapeutic effects of conventional TMS protocols are relatively weak and variable [15–18, 38–41]. In experimental brain research, the weak and variable effects necessitate large subject populations to establish sound group effects; in treatment, however, they limit the efficacy on the individual level [12, 38, 40, 42].

Recent coil designs have pushed the spatial selectivity, i.e., focality, to its limits [9]. As pointed out there, this limit is associated with the nonnegligible coil-to-cortex distance as electrodynamics does not allow a focus in depth for the near-field of the TMS coil, where the head resides. Despite the spatial limitations, however, there is mounting evidence that

the temporal shape of TMS pulses affects the functional selectivity of neural stimulation as well as the direction and strength of neuromodulation [37, 43–60]. For example, monophasic TMS pulses produce stronger and more selective neuromodulation than biphasic pulses [61–66]. However, the way conventional technology generates monophasic pulses is highly inefficient. The second half of the current pulse is generated through resistive damping so that the entire pulse energy is converted into heat (see Figure 1) [67]. In consequence, existing TMS devices cannot generate conventional monophasic pulse trains at rapid rates, with few exceptions that were never deployed widely due to their excessive power demand [8, 68]. The use of standard monophasic pulses, as just one example of alternative waveforms, is limited to few applications and pulse protocols. Clinical treatments, however, are exclusively performed with so-called biphasic pulses, which have inferior efficacy and selectivity [18, 69–72].

Other pulse shapes have been shown to provide activation selectivity, increase the neuromodulation efficacy of pulse trains with that pulse shape, or affect physical features of stimulation, such as coil heating or sound emission. Various asymmetric near-rectangular pulses were shown to increase selectivity and produce stronger neuromodulation effects with similarities to conventional monophasic pulses [43]. Varying the pulse symmetry and pulse duration furthermore apparently allows shifting of the activation balance between different neuron populations [44–48, 57, 59, 60, 73, 74].

Stimulation with pulses of different durations demonstrated that pulse shapes also affect a subject's or patient's perception of the pulse on the scalp, likely due to the different activation dynamics of nociceptors and other sensory fibers in the skin compared to the various cortical neurons [75]. Pulses with the majority of their spectral content in higher frequency ranges emit less sound, which is more than just a technical nuisance and artifact of TMS as it concurrently stimulates auditory circuits [76–81]. The loud clicking sound of pulses could previously not be isolated from the electromagnetic stimulation and is always exactly in sync with it. This confounds TMS studies and clinical applications because auditory stimulation is known to have a strong neuromodulatory effect on brain stem and/or neocortical circuits [77, 82].

Beyond the physiology, optimized pulse shapes allow reducing the heating of TMS coils, which traditionally limits repetitive TMS protocols and has to be kept within certain limits for safety reasons [83–86].

Finally, the ability to change the TMS pulse shape can enable analysis of the stimulated neuron population and its activation characteristics, e.g., through identifying the first order of its dynamics, which, beyond distinguishing between various targets, may allow diagnosis of various diseases [73, 87, 88].

Regrettably, the temporal aspect of the TMS stimulus cannot be explored and optimized fully because existing technology has fundamental limitations of the ability to control the shape and sequences of the induced electric field pulses. To exploit potentially increased selectivity, neuromodulation strength, and energy efficiency of optimized stimulus waveforms, there is a need for a TMS device that allows flexible synthesis of pulse shapes

and sequences. An unconstrained experimental search and application of optimal waveforms with respect to activation selectivity, strength, and reliability of various neuromodulation techniques, as well as physical aspects, such as pulse sound emission or coil heating, would require a device and circuit technology that allows the generation of practically any pulse shape and any sequence.

Existing Device Technology

Available devices and pulse shapes

In conventional TMS devices, the coil voltage pulse, and hence the electric field waveform, has a damped cosine shape [89]. Most commercial devices offer a selection of biphasic and monophasic sinusoidal current pulses with very limited control over the pulse shape and width [50, 90–92]. These devices exclusively implement high-voltage oscillator circuits, which are charged up slowly and release the energy rapidly through oscillation between a pulse capacitor and the stimulation coil, activated by a high-voltage high-power switch (Figure 1A, B) [89, 91, 93]. The oscillation is either terminated typically after one period to retrieve some of the pulse energy (biphasic TMS) or over-damped to zero, in which case the pulse energy is dissipated as heat (monophasic TMS). In contrast to monophasic TMS, biphasic devices do not intentionally use any damping resistor to shape the pulse and can recycle a large share of the energy in the pulse capacitor after a pulse and only replenish the loss through a power supply [94]. Changing the pulse shape requires rewiring of the circuit, e.g., by increasing the capacitance or adding damping resistors, but is technologically cumbersome and practically yields only a handful of pulse options with limited repetition rates [50, 53, 58, 95–98].

We previously developed controllable pulse parameter TMS (cTMS) to address some of these limitations of conventional TMS devices [96, 99–101]. cTMS and related approaches, such as flexTMS [102, 103], use switching between one or two oscillators with large capacitors to enable electric field pulses with nearly rectangular shape and some control over the pulse width and, in some cases, the amplitude ratio between the positive and negative pulse phases (Figure 1C) [96, 100, 104]. Coupling various capacitors and inductors has been suggested to bring pulse-shape flexibility [105–108]. However, these devices are still very limited in their pulse shapes and also cannot generate conventional sinusoidal pulses, such as the traditional monophasic or biphasic waveforms, for comparative studies or to perform already approved clinical procedures [96, 99, 100, 102].

These technological limitations of existing TMS devices stem from several factors. Fundamentally, high energy and power levels as well as fast pulse dynamics are required for transcranially evoking action potentials in cortical neurons through electromagnetic induction. This necessitates TMS devices to employ high voltages (often even up to 3,000 V), large currents (up to 8,000 A), and fast switching (< 1 μs) [2, 5, 53, 93, 109–111]. To handle these extreme requirements, existing TMS devices exploit simple but inflexible circuit topologies, usually one or several oscillators, and high-power but slow semiconductor switches (thyristors in conventional TMS and insulated-gate bipolar transistors (IGBT) in later devices) [100, 112–115].

In the devices discussed above, the pulse shape or family of pulse shapes are still very characteristic for the specific stimulator circuit. A practical technology to generate relatively freely almost any existing and user-defined pulse shape would have to use a single flexible and efficient circuit topology. For example, if that technology could generate pulses without the need for deliberate damping with resistors, it would allow the generation of monophasic pulses with energy loss and coil heating comparable to biphasic pulses [83].

Limitation in combining various pulses in sequences flexibly and efficiently

No conventional single TMS device allows controlled changes of the pulse amplitude and pulse shape between two or more pulses delivered in rapid succession. Such rapid changes are, for example, relevant for paired-pulse measurement protocols, conditioning pulses, or interleaved modulation and probing pulses [51, 116–119]. Several devices can be combined to feed a single coil with pulses to rapidly change the pulse shape or just the amplitude from one pulse to another. However, for every different pulse shape class or amplitude involved, a separate device is necessary. The inability to alter the pulse amplitude rapidly results from the circuit topologies of conventional devices, which do not allow rapid changes of the voltage of the energy storage capacitor that determines the pulse amplitude. Such limitations also apply to existing TMS devices using various bridge topologies (e.g., Figure 1C), including a restricted set of pulse shapes that can be sustained in repetitive trains as many pulses transfer charge from one capacitor to the other; inability to combine different pulse shapes or amplitudes in a sequence or a train; and suboptimal energy losses and coil heating [96, 99, 102]. In conclusion, there are multiple technological limitations of existing devices that impede the exploration or adoption of stimulation protocols that could enhance TMS applications.

Limitations for generating any user-defined pulse

Various approaches have been implemented or proposed to increase the flexibility of pulse shaping by relatively rapid switching of the coil during the pulse. Some used conventional voltage-source inverter circuits with bridge configurations of transistors, typically IGBTs [120], which are known for example from motor inverters of electric vehicles [121, 122]. The bridge circuit switches the voltage of the coil rapidly between a small number of voltages (typically positive supply, negative supply, and zero voltage) to generate an approximation of a reference current shape. Current-source alternatives were considered but might provide less flexibility in TMS [123, 124]. Half-bridge or so-called chopper arrangements with switching modulation share the circuit topology with the first version of cTMS [100, 101]. In contrast to full bridge configurations, they switch between two voltages (on and off) to generate unipolar current pulses.

Thus, power electronic inverters have been evaluated early on as a solution for shaping the TMS coil current, and this concept has been revisited several times since then [125, 126]. However, the use of conventional inverters for TMS pulse shaping has significant problems. A few transistors have to manage three challenges at the same time: the full pulse current (as all the current of several kiloamperes is flowing through them), the maximum voltage (as the same transistors have to block the entire pulse voltage of several kilovolts when turning off), and the full bandwidth, i.e., frequency content and dynamics of the pulse

(kilohertz range), which overwhelm practically any available power semiconductor. In short, the IGBTs of a conventional inverter have to switch the full pulse currents fast (e.g., < 1 μs, to avoid large energy loss during switching at these high current levels) and frequently (e.g., > 50 kHz, ideally notably more, at least a decade above the highest frequency content of the intended pulse for sufficient usable frequency bandwidth in pulses without large harmonics where neurons might be sensitive) while they need to block the entire voltage. In conventional TMS devices, the semiconductor switches—typically thyristors— are overloaded with currents multiple times their continuous ratings for the short duration of a pulse. Overloading is not only a means to cut semiconductor switch costs, but it reduces the parasitic properties of the semiconductor devices, such as the capacitance and other charge-storing effects as well as associated reverse recovery, and therefore allows faster switching speed. IGBTs can also be overloaded, but not as far as thyristors. Furthermore, the stress of TMS-level currents on transistors is enormous when they have to perform hard commutation at the same time. High-voltage IGBTs are moreover rather slow compared to the spectral content of TMS pulses and lossy in switching. Consequently, in contrast to motor inverters, where the switching frequency is orders of magnitude higher than the generated waveforms, IGBTs can only switch a few times per TMS pulse.

Most importantly, the current shape, which such inverters control as required for motors and which appears relatively smooth, is not directly relevant for the stimulation effect of TMS. Instead, the stimulation effect of TMS is mediated by the induced electric field. The electric field is proportional to the coil current rate of change and hence approximately follows the coil voltage time course. Since the TMS coil voltage switching is performed between the available supply voltage levels, which usually are in the kilovolt range, the electric field in stark contrast to the apparently smooth current has a high-amplitude rectangular pulse waveform. Consequently, the neuronal membrane potential, which is driven by the induced electric field, experiences a high-rate burst of ultra-brief sharp-edged pulses with varying pulse duration in the range of microseconds or tens of microseconds, each pulse in the burst with maximum stimulator amplitude. These durations lie in the range of individual pulses previously successfully used for neurostimulation [73, 100, 127, 128]. Since the active neuronal membrane is nonlinear, such pulses have a different physiological impact than pulses with a more continuous electric field waveform, such as those of conventional TMS pulses. Indeed, the strong nonlinearity of neurons is relevant particularly for short pulse durations and high amplitudes [129–132]. Thus, while novel TMS pulses with high-frequency content may be an interesting parameter space to explore, such inverter circuits cannot reproduce standard TMS pulses or synthesize other pulse waveforms with a continuous electric field profile.

We previously argued that a conventional inverter circuit cannot provide at the same time the quality, power, and bandwidth necessary for flexible TMS pulse synthesis, and introduced alternative circuits; these circuits split the high voltage, current, and switching frequency into smaller, manageable portions distributed over many faster, lower-power semiconductor devices [133–139]. We developed as well as tested the principle in various stages and recently used a simplified implementation with older semiconductor technology to reduce the sound of TMS pulses through different coil structures and pulses with dominant frequency contents above the hearing range [76, 80, 140]. The system distributes

the necessary high voltage above 10 kV among many lower-voltage transistors but uses rather slow IGBT semiconductors so that only few switching transitions during a pulse are possible. In combination with the large voltage steps, only very limited reproduction and imitation of existing as well as future pulses is possible, while the deviations are substantial. Furthermore, the device cannot offer rapid sequences of equal or even very different pulses.

In this paper, we present a modular pulse synthesizer TMS device (MPS TMS) that uses a modular circuit topology combined with the latest fast-switching unipolar field-effect transistors using wide-bandgap silicon-carbide semiconductors. The latter exhibit less slow charge-storage effects than silicon IGBTs or super-junction field-effect transistors, permitting rapid switching at high power. The combination of a modular circuit topology and fast semiconductor switches enables a TMS device that can generate practically any pulse shape, including the existing ones, with high output quality of the induced electric field. The high pulse shape flexibility allows generating user-defined pulses with only a few constraints, such as a maximum voltage, current, frequency bandwidth, and duration, as well as the current returning to zero at the end of the pulse. Furthermore, since the synthesis of pulses becomes a digital control problem, and therefore a software task, practically any set of various pulse shapes, durations, directions, and amplitudes can be combined into rapid pulse sequences without the need to mechanically reconfigure the circuit or slowly change the charge level on capacitors between pulses as in available devices. For example, MPS TMS can synthesize conventional monophasic pulses accurately with energy recovery after a pulse to enable high efficiency and also high repetition rates—a feature that has been technologically limited to biphasic pulses [133]. Furthermore, since MPS TMS can generate existing pulses with high fidelity, it could equivalently generate FDA-approved treatment protocols.

Modular Circuit Topology

As introduced above, TMS pulses challenge power electronics, specifically due to the simultaneous occurrence of high power (currents of typically 5–10 kA, high voltage up to ~ 3 kV peak to zero) and high dynamic range ($\gg$ 10 kHz, with low distortion at least > 100 kHz; often desired sharp transients in the pulse requiring notably more), which requires fast switching or circuit reconfiguration for free control. In conventional circuits, such as choppers, half bridges, or full bridges, individual power semiconductors have to manage high current, voltage, and frequency bandwidth at once. Available semiconductor technology may achieve each of the three requirements alone.[1] To date no semiconductor type can satisfactorily manage all three, high current, voltage, and bandwidth, without compromises at the same time.

Even if new devices, such as wide-bandgap semiconductor IGBTs, may allow it in the future, the rectangular electric field would, as outlined above, generate mostly rectangular pulse bursts. Without a large high-power filter between the power electronics and the

---

[1]High-electron-mobility transistors for fast switching in the megahertz range may allow the bandwidth but have insufficient voltage and current capability; high-voltage high-current IGBTs on the other hand are available for mega-volt-ampere (MVA) of power but their large parasitic inductances and capacitances as well as slow bipolar charge-carrier dynamics limit the bandwidth and introduce distortion already at low frequencies.

coil, these bursts would not resemble the desired smooth pulse or be equivalent to any conventional pulse shape.

We combined two ingredients to solve this problem. First, we designed a circuit class that splits power and switching into smaller, manageable portions [133–136]. Figure 1D depicts the circuit topology as a string of modules, which jointly generate the output. Each of these modules contains its own capacitor and transistors, which only need to deal with a fraction of the pulse voltage. Second, we adopted fully unipolar field-effect silicon-carbide (SiC) transistors. These SiC transistors avoid the issues of other semiconductor devices; specifically, the SiC transistors escape the slow dynamics of minority carriers in pn junctions of bipolar devices such as thyristors and IGBTs as well as the large charge-storing effect in the voluminous drift zone of high-current super-junction silicon field-effect transistors and their large diode reverse recovery due to necessarily high doping levels [141–145]. Slow IGBTs or superjunction transistors in the modules could limit switching or circuit reconfiguration to only few times during a TMS pulse as in previous more flexible TMS devices, leading to substantial deviations if they try to approximate a smooth pulse.[2]

Accordingly, a number of lower-voltage modules contribute their individual lower power and lower switching dynamics to generate a more powerful and faster output for a TMS pulse. The lower voltage in each module allows the use of lower-voltage components for capacitors and transistors with faster switching dynamics. At the same time, if appropriately coordinated, the overall switching is likewise distributed and temporally shifted among the individual modules so that each module only needs to deal with a fraction of the switching speed to achieve overall effective switching rates approaching the MHz range. Similar to the voltage, the individual modules further only change the output electric field in small steps so that they have fine control over the field amplitude in stair-case fashion, which switching modulation can smoothen further. Due to the low amplitude and high frequency of the steps, the energy content of the distortion product is small and falls below 0.1% of the pulse energy. With sufficient distance of the distortion spectrum from the highest pulse spectral content and due to the low energy content, compact filters can in principle eliminate such distortion if needed.

Each individual module forms a local dc voltage supply with a storage capacitance and contains several transistor bridges. The transistor bridges connect the module to the neighboring ones or the stimulation coil (see Figure 2). The capacitors are charged before a pulse starts. The transistors allow rapid reconfiguration of the overall circuit: by appropriate activation and deactivation of transistors, the module capacitors can be included into the coil-driving circuit with either polarity or bypassed, effectively increasing or reducing the output voltage supplied to the stimulation coil within a microsecond. A circuit with N modules and similar capacitor voltages can step the output voltage with $2N + 1$ steps, i.e., $-N$, …, 0, …, N. As in any TMS device, the current is almost entirely inductive and therefore follows approximately the time integral of the output voltage. Any switching modulation to generate intermediate steps can be performed exclusively with the size of one

---

[2]A 10 kHz switching rate, for instance, would amount to only switching two to three times during a 200 μs pulse and four to five times during a 400 μs pulse after all, which may clarify why the resulting approximation can be very coarse.

voltage step. The small steps are a fundamental advantage of the proposed configuration in contrast to the afore-mentioned conventional power inverters.

The module circuit preferably contains four individually controllable transistor bridges in each module so that a module is connected to each of the adjacent modules through two interconnections. This pairwise interconnection allows module capacitors not only to be dynamically connected in series to the other included capacitors but also in parallel for balancing charge or sharing load [135]. The extra bridges appear to double the number of transistors needed. However, all transistors share load and the circuit achieves the same semiconductor utilization. Thus, the individual transistors in the four transistor bridges, each of which nevertheless aggregates several parallel transistor dies, can have only half the current rating so that the overall power semiconductor amount is the same for two or four transistor bridges, while the opportunities for control increase [146]. Furthermore, the bridges can act in parallel so that the four-bridge module can operate equivalently to a two-bridge module with the exact same performance. Table I compares these options of the technology.

The overall circuit is furthermore symmetric. Although the device can generate pulses the same way as conventional stimulators, the circuit symmetry further allows generating pulses differentially. Differential pulse generation means that the machine feeds the two coil terminals with inverse voltages (relative to ground) so that the average electric potential of the coil, i.e., the voltage versus ground averaged over the entire coil and in figure-of-eight coils also the important center in the middle of the two wings as the location being closest to the head, stays close to zero throughout the pulse. Conventional devices, in contrast, generate pulses exclusively in a single-ended style, where one coil terminal is fixed, often grounded, and the pulse voltage that drives the current through the coil is solely generated through the other terminal. As a consequence, the average electrical potential of the coil fluctuates throughout a pulse with rather sharp edges. Such electrical potential fluctuations on the order of thousands of volts within microseconds turn the coil into an antenna and generate strong capacitive interference in sensitive electronics nearby. This interference is part of the stimulus and therefore synchronous with it. Thus, it leads to artifacts in recording equipment for neural signals, particularly electroencephalography (EEG), which is not easily separable and often saturates the amplifier so that the amplifier is insensitive to neural signals right after a stimulus [147].

The modular circuit allows various ways for recharging both on the module level with charging each module independently or only a few of them in combination with a charge distribution through the power loop. Alternatively, charging can also occur entirely on the system level by distributing a voltage to the module string through the power loop. The implementation described below charges through a dc supply to the capacitor of one module, from which the power is supplied to the others via the parallel channel offered by the four-bridge modules.

Control and Balancing

The modules collectively and dynamically reconfigure the series and parallel configuration of module capacitors presented to the stimulation coil. The various options of how modules can interact and form the dynamically changing overall circuit is best represented and controlled by so-called module or interconnection states [148]. The four-bridge module topology has four interconnection state types (Figure 3): Specifically modules can (1) dynamically connect in series plus (i.e., stepping up the voltage in positive direction) and series minus (i.e., stepping down the voltage in negative direction), which insert the module's capacitor into the coil loop in series with the others with either polarity; (2) the bypass state disconnects the module capacitor from the pulse current by guiding the current around; (3) in the passive state, all transistors are turned off so that only the free-wheeling diodes act as a rectifier from the module terminals towards the module capacitor; (4) various parallel states—typically one is sufficient—can connect the capacitor in parallel to one or more other module capacitors. Two-bridge modules can only generate the subset of series plus, series minus, bypass, and passive, while the parallel configuration is not possible.

In contrast to conventional TMS devices, the control has to implement several functions. It has to translate a specified continuous electric field or current shape into a quantized representation that uses the fine amplitude granularity and temporal switching speed of the system, decide which transistor in the system has to switch on or off at which point in time, and balance the load so that each module is delivering similar charge, similar power, and a similar share of the switching load [149].

In the first approximation, the output voltage $v_{\text{coil}}(t)$ is the sum of the module capacitor voltages $v_{\text{m},k}$ that are in one of the series states per

$$v_{\text{coil}}(t) = \sum_k s_k v_{\text{m},k}(t),$$ (1)

assuming $s_k(t)$ represents the state for the k-th module or interconnection according to

$$s_k = \begin{cases} +1 & (\text{ Series } +) \text{ if } m \geq C_k, \\ -1 & (\text{ Series } -) \text{ if } m \leq -C_k, \\ 0 & (\text{Parallel or Bypass}) \text{ otherwise.} \end{cases}$$ (2)

The modulation method we preferably use is based on phase-shifted carrier modulation, PSC (Figure 4), which can perform modulation, scheduling, and balancing with appropriate design [150, 151]. As shown in the top panel of Figure 4, the modulator generates a set of k cyclic triangular carriers $C_k(t)$, each in two polarities and shifted against the others in phase to temporarily interleave switching of the modules for a high effective switching rate. Each carrier pair (carrier and its inverted version) corresponds to a module. The switching signals are determined by comparing a pulse shape reference $m(t)$ with the individual carrier pairs in size (bottom panel of Figure 4): If the signal is larger than both carriers of a pair, the output is +1; if it is smaller than both, the output is −1; if it is between them, the output is 0. The comparison result (+1, −1, or 0) is conveniently the module output state s_k for the corresponding module. The PSC modulation determines the switching rate by its carrier

frequency. Since the carriers are evenly shifted in phase, the effective switching rate at the TMS output is $N f_{\text{carrier}}$, e.g., with $f_{\text{carrier}} = 50 - 100$ kHz and $N = 6$ modules. PSC rotates states through all modules so that the modules get loaded similarly. Proper choice of the carrier sequence can furthermore exploit the opportunities of the parallel mode for charge balancing across modules as well as to reduce conduction loss [150, 152]. Other modulation techniques are possible and described in the literature but are designed for the typically notably slower switching rates and output bandwidth (typically < 1,000 Hz) as common in power conversion applications and therefore often generate a substantially higher computational burden or lower-frequency distortion [153–159].

The pulse reference shape $m(t)$ preferably describes the normalized (between −1 and +1) pulse shape through its voltage over time. This pulse reference shape m can be derived from the coil voltage profile desired by the user or since the coil and circuit parameters are known also indirectly from the coil current i_{coil}^*. As a first approximation, m can be formed in an open-loop control approach as $m(t) = v_{\text{coil}}(t)/(N v_{\text{m}})$ for N modules with equal and constant module capacitor voltage $v_{\text{m}} = v_{\text{m},k}$. If the reference is given as a coil current i_{coil}^*, setting

$$m = \frac{1}{N v_{\text{m}}} L \frac{\text{d}i_{\text{coil}}^*}{\text{d}t} \tag{3}$$

produces a very close approximation of the reference (see Figure 5A). However, during the pulse, the capacitor voltages can change and deviate from each other, while the inner resistance R_{i} of the circuit, cables, and the coil absorbs some of the output voltage before it reaches the inductance of the stimulation coil and therefore distort the pulse.

Conventional closed-loop control during a pulse, which would be the solution in conventional power electronics to compensate such deviations, is not recommended as extremely fast feedback would be necessary for the current and voltage dynamics of TMS. Instead the pulsed application allows a closed-loop control scheme from pulse to pulse to adjust parameters. If detailed circuit parameters are known, e.g., measured beforehand, we can pre-compensate the change of the module dc capacitors and the stray resistance in m, as in

$$m = \frac{1}{N v_{\text{m}}(t)} \left(i_{\text{coil}}^* R_{\text{i}} + L \frac{\text{d}i_{\text{coil}}^*}{\text{d}t} \right). \tag{4}$$

Equation (4) adds the ohmic voltage drop to the modulation reference and considers the discharging effects of the module capacitor voltages (accounting for capacitor energy e_C, coil energy c_{coil}, Joule loss e_R, and output energy e_{out}), which are represented by the time dependence of $v_{\text{m}}(t)$.

The improvement is obvious when compared to the uncompensated standard PSC as is shown in Figure 5 ($L_{\text{coil}} = 9$ μH, $R_{\text{i}} = 36$ mΩ, $C_m = 3.6$ mF, $N = 6$, no parallel state). Both methods leave a noticeable module voltage spread on the order of 5 V at the end of the pulse as the control does not use the parallel mode there. Parallelization, as uniquely offered by the four-bridge modules (see Table I), clears such voltage differences. It can generate loss (E_{loss}

$= ¼ \, C_\mathrm{m} \quad V_\mathrm{m}^2$) but if done regularly, e.g., instead of every bypass state during a pulse, can be negligible [135]: both examples produce < 50 mJ balancing loss while the overall energy loss can exceed 50 J. Model-predictive control, which estimates the future during control, can further reduce loss and deviation from the reference, but does not appear necessary for fundamental operation [157].

We furthermore added a formalism that allows adding more advanced balancing to the control, which can eliminate also the above small balancing loss. The individual references of the modules are modified with additive terms (m_k for module k with $\Sigma \; m_k = 0$) that collectively add up to 0 at each time to achieve even closer module voltages than the balancing capabilities of PSC modulation. The modified composite modulation reference ($m + m_k$) exactly corrects the deviation from the average discharge of each module. Figure 6 demonstrates the balancing improvement.

As the device can generate pulses very freely, including so far unknown and even user-defined pulses, the control has to enforce constraints that are naturally fulfilled in conventional technology due to its limitations. In addition to maximum current amplitude and charge levels per phase, these constraints also include that a pulse does not end with non-zero current. As the current is the solution of a differential equation representing the circuit excited by the modular pulse synthesizer, the control has to estimate the current at the end of the pulse ahead of time to avoid substantial residue magnetic energy in the stimulation coil associated with nonzero current at the end of the pulse. The passive state of the modules or module interconnection can serve to recycle such residual energy at the end of a pulse [133]. The passive state uses the diodes of the modules so that residue current of any polarity is rectified into the modules to charge the capacitors. It can be actively controlled in its voltage amplitude by replacing series states with passive ones and combining them with bypass or parallel states statically or preferably in switching modulation to set the discharge time course.

Implementation

We implemented the technology with six modules, each with four power half bridges to have access to parallel module interconnection states (see Table II for key components). Each module was implemented with 24 discrete SiC transistors (FF11MR12W1M1, Infineon, Germany, with press-fit circuit-board connection) to enable peak currents of at least approximately 8,000 A and voltages up to at least 4,000 V (peak to zero). The transistor and the included dies were tested for their channel saturation current level for various gate voltages to evaluate the transient over-load potential. In contrast to conventional TMS devices, the power circuit did not use a hand-wired setup of discrete components but heavy-copper printed circuit boards (PCB) that represent the identical modules. The four-layer PCBs (2×75 μm and 2×105 μm copper) contain the SiC transistors, gate drivers, three levels of capacitors to allow fast switching without large voltage spikes, and module-level control electronics (see Figure 7). The PCBs are furthermore designed to fit into 19" racks. The pulse current is routed on the PCBs on all four copper layers in a laminated style for minimum parasitic inductance.

As the most critical component, we thoroughly optimized the switching cell, i.e., the high- and low-side transistors of a bridge together with their physical current routing. We placed a first-stage module capacitance and the gate driver in close vicinity with minimum inductance and coupling to enable rapid switching of the high TMS pulse currents. Following the switching cells, the entire module capacitor bank is split into three parts or stages with increasing distance and therefore parasitic inductance. The three stages serve different key purposes and use capacitors with smaller, lower inductance, and faster-responding capacitors closer to and higher energy content farther away from the transistors. The first stage capacitance, as part of the switching cells, is small, mostly stores the charge during commutation, and absorbs the load current during that time. For sufficient response dynamics, it is formed by low-inductance, low-resistance surface-mount ceramic capacitors (B58031U9254M062, EP-COS/TDK, see Figures 7 and 8) with 12 μF per module and provides and/or absorbs the immediate energy needed to discharge the magnetic field of the current path on the PCB before switching and to charge the magnetic field after switching. To further minimize those energies, the current path is routed for minimum commutation stray inductance, i.e., such that the current before switching and the current after switching share almost the same path and direction so that they can take over the magnetic field of each other. The individual switching cells were assigned to output bridges of the module in an interleaved manner for minimum inductance and best current balancing performance (see Figure 8). Gas discharge tubes (CG21000L, Littelfuse, Illinois, USA) across the module dc bus (and thus the capacitors) protect the switching cells against overvoltage and can absorb high energy levels.

The gate drivers (1EDI60H12AH, Infineon) are mounted on the other side of the PCB, underneath the corresponding transistors and supplied by compact dc/dc converters (MGJ1D121905MPC-R7, Murata, Japan). We switched the transistors with gate–source voltages of +19 V/–5 V to achieve (1) minimum conduction loss in the transistors, (2) fast turn-on/-off transients, (3) suppression of spurious turn-on events in response to capacitive as well as inductive interferences, and most importantly (4) to shift the transistor channel saturation to allow higher current levels. The gate and corresponding source signals were routed as parallel differential pair with minimum distance to the transistors with less than 25 mm trace length and connected with a Kelvin connection to the transistors. The Kelvin connection avoids large potential shifts in the gate-drive reference due any voltage drops generated by the large load current.

The second-stage capacitance is a larger intermediary formed by low-inductance metalized film capacitors with 194 μF per module (C4AQQBU4270A1XJ, Kemet, South Carolina, USA). The third-stage capacitance with 1.8 mF per module is farthest away from the switching cells with the largest capacitance to provide the major pulse energy but contributes little to commutation (C4AQQBW5300A3MJ, Kemet). Each module further contains a discharge unit, which can decrease the module voltage and also rapidly bring the device into a safe state (i.e., below safety extra-low voltage, SELV) in case of unexpected events or failures. The discharge unit contains high-reliability normally-on reed relays (DBT71210U, Cynergy3 Components, England, UK) and discharge power resistors (AP101 470R J, Ohmite Manufacturing, Illinois, USA). The controller only opens the relays to

allow charging after a successful self-test. The modules are connected with copper bars and alternate their position for close-to-ideal current sharing.

Each module contains a complex programmable logic device (CPLD, MAX10, 10M02SCE144I7G, Altera/Intel, California, USA), which coordinates all fast processes such as switching, and an ARM-based microcontroller (ARM M4, MSP432P401RIPZR, Texas Instruments, Texas, USA, Arm, Cambridge, UK), which monitors the module, e.g., the temperature sensors. Both controllers can watch each other through hand-shake signals for proper operation and to identify failures. The overall control is performed on a central level by a system-on-chip controller (NI sbRIO 9627 with AMD/Xilinx Zynq 7000) and commands all module controllers through a bus system. The bus is isolated from the modules through signal isolators (ISO7841FDWW, Texas Instruments) and line drivers (UCC27712QDQ1, Texas Instruments).

Performance

Switching and thermal performance

The major challenge for dynamic pulse shaping is rapidly switching the high TMS pulse currents from one physical current path to another (commutation). As the current paths before and after a switching action cannot be perfectly identical, their magnetic fields and associated energy content differ. When these energies dissipate electrically in an uncontrolled manner, they lead to voltage spikes when the current is handed over between low-side and high-side transistor, which can damage the semiconductors. We performed double-pulse measurements through pumping an inductor (in this case, TMS coil D70, Magstim, Wales, UK) through the module as outlined in Figure 9 to form a triangular waveform and monitoring switching for all four conditions (commutation from high-side to low-side and from low-side to high-side for inwards and outwards current). A digital scope (Tektronix MDO3054, Oregon, USA; 500 MHz bandwidth) with voltage probes (Tektronix THDP0100; 100 MHz bandwidth) and Rogowski sensors (PEM CWTMini HF, UK; 30 MHz bandwidth) served for the measurements. The voltage was measured at the pins of the transistors and could be kept within the specified range up to transistor channel saturation. An optional but not necessary modification of the transistor casing can reduce the parasitic inductance of the transistor itself and reduce voltage spikes for this application (Figure 10).

Furthermore, the power electronics underwent stress testing with repetitive pulses to evaluate thermal limits under various switching conditions (see Figure 11). The test pulse current profile was bipolar sinusoidal with various pulse durations and peak levels of $\pm$ 700 A per discrete transistor. In each condition, the module performed approximately a million pulses to reach steady-state conditions of the (after all temperature-dependent) electrical and thermal conditions. The results in Figure 11 demonstrate that switching of up to 100 kHz per module is well within the performance range of the design so that six modules can safely reach an effective switching rate of 600 kHz.

Synthesis of all conventional pulses with energy recovery

Figure 12 shows three biphasic pulses with sinusoidal current and cosinusoidal voltage shape with varying pulse durations. The electric-field pulse shape as the derivative of the current in the stimulation coil follows approximately the voltage shape if the inner resistance of the high-current loop formed by the electronics, cables, and the coil is low. The generation of the pulse shape is fully controlled throughout the pulse and does not depend on any hardwired oscillator of a pulse-shaping circuit in conventional devices. Thus, the device can easily change the pulse duration as demonstrated in the figure. Compared to cTMS as the first TMS technology that could also rapidly change the pulse duration through software by actively terminating phases of an oscillator, the pulse does not have to be rectangular, but may be sinusoidal or have any other shape. The setup can provide sufficient voltage for short pulses, which need higher amplitude for stimulation, and energy for exceptionally long pulses with their large charge content per phase (Figure 12 C).

As a consequence of this software generation, the pulses also do not exhibit the typical amplitude reduction of some 20% of conventional biphasic TMS devices from the beginning of the pulse to the end, but the pulse voltage can end with the same amplitude as it started. In conventional devices, the amplitude reduction is a consequence of the energy loss in the oscillator; the conventional oscillator starts with a specific pulse energy and depletes throughout the pulse, resulting in decaying current and voltage amplitudes. The synthesizer does not have any such constraints so that the pulse can have constant amplitude over time, although it could imitate such damping.

Naturally, the device can generate other conventional pulse shapes, such as just half a period of a sinusoidal current and cosinusoidal voltage, sometimes called half-wave pulses (see Figure 13), and monophasic pulses (see Figure 14). As was already pointed out in our previous descriptions of the technology, the circuit does not contain any resistors for shaping a pulse [133, 134]. The abandonment of any resistance for pulse shaping, which is essential in conventional monophasic TMS devices and responsible for most of the problems of the pulse shape, has substantial impact: As a consequence of the energy recovery and the low energy loss even in monophasic pulses, the technology can generate monophasic pulses at repetition rates of 50 Hz and higher. As outlined below, the device can even synthesize pulses in rapid pulse trains with practically no time between pulses or mix them with other pulse shapes in a pulse train. The decay phase of the monophasic pulses, which conventional monophasic stimulators generate by connecting a powerful resistor to the coil and in which they convert the entire pulse energy into heat, is entirely simulated here only. The pulse synthesizer extracts the current of the coil so that the current decays with exponential shape and the voltage exhibits only a shallow low-amplitude counter-phase as intended. From the perspective of the coil, the machine thus still shows apparently resistive behavior, but the energy is widely recovered instead.

The device technology can use two ways to adjust the amplitude of a pulse. It can change the voltage of the modules, which changes the voltage step size and thus the granularity. In addition, the controller can modulate, i.e., calculate how to coordinate the modules to use the available voltage steps to generate the output at a different pulse amplitude. For lower amplitudes of the same pulse shape, it can, for instance, use fewer module steps. Fewer

module steps, however, can decrease the output quality as the granularity becomes coarser and thus should be used only cautiously (see Figures 12 and 14).

Generation of novel and user-defined pulses

Since pulse shaping is entirely a programmable control issue and performed by embedded software, the technology and its presented implementation can generate a wide range of pulse shapes with only few technological constraints, such as peak current, peak voltage, charge per phase without current reversal, and zero current at the end of the pulse. Importantly, due to the principle of the circuit, it generates all pulses without any exceptions with energy recovery, which previously was only known from conventional biphasic pulses.

Figure 15 demonstrates the ability of the device to deviate from the beaten track and generate unconventional pulses. The recording combines more conventional monophasic pulses with reversed ones, which no conventional TMS technology could possibly generate as the pulse now practically starts with a quasi-negative-resistive damping phase, which increases the pulse amplitude.

Polyphasic pulses, i.e., pulses with more than one sinusoidal current period were among the first in TMS and are promoted for special applications to this day due to their increased stimulation strength already at lower voltage and current amplitudes and under certain conditions presumably lower sound emission [92, 94, 115, 160, 161]. Conventional polyphasic technology, however, needs to use oscillator circuits so that the pulse amplitude is constant or rather falls during the pulse due to damping. Figure 16 instead shows pulses of sinusoidal currents with Gaussian envelope with varying width. Thus, the current oscillation builds up from an initially small amplitude below the noise floor to reach a maximum and subsequently decays again. For very short envelope widths, the pulse degenerates into a biphasic pulse with near-sinusoidal current but in contrast to conventional biphasic TMS pulses smoother leading and trailing edges in the voltage and the electric field. Neither the increasing amplitude during the first half nor the decay without damping is possible with conventional TMS circuitry or modifications of it. In Figure 17, the carrier wave under the Gaussian envelope is a cosine current. This pulse degenerates to a sinusoidal voltage for very short envelope widths.

As another example of a pulse that conventional devices cannot generate, Figure 18 displays recordings of a loss-optimized biphasic pulse type that generates less coil heating than any standard pulse with adjusted stimulation strength as found previously [83, 84]. This pulse type includes a shallow pre-phase before the actual pulse, which has almost negligible electric field and therefore little influence on the neural activation. However, it generates an offset in the current baseline so that the current can subsequently contain a longer rising edge without reaching large current amplitudes. As the heating in the coil is mostly proportional to the squared current, the reduction of the peak over-compensates any loss of that pre-phase. Again, the already emphasized capability of the system to retrieve the pulse energy not only enables reducing coil heating with this pulse but furthermore also exploit the potential to reduce overall pulse losses in rapid trains.

Figure 19A presents the amplitude spectrum of a biphasic pulse generated by the device. The measurements are without any filter to catch a wide range of the spectrum. As biphasic pulses are mostly sinusoidal current and cosinusoidal voltage pulses, they show a dominant frequency corresponding to the period length. Due to the cut-out of only one period, however, the maximum is broad. Furthermore, the intended sharp start and end of the pulse leads to strong inherent side bands in any biphasic pulse, which mask potential distortion, i.e., the deviation from the desired perfect sinusoidal shape due to the quantization—visible, for instance, in Figure 12. Figure 19B therefore additionally displays the spectrum of a longer bandwidth-limited polyphasic pulse with smoother Gaussian envelope, sharper spectral maximum, and no side bands to make the distortion better visible, which emerges out of the measurement noise near the frequency axis at higher frequencies of the voltage spectrum. In the current spectrum, the distortion is as expected less noticeable due to the inductive nature of the coil, which presents a high impedance to high-frequency contents. The amplitude of the distortion (and more so the power content) particularly of the voltage is only a fraction of the dominant frequency components of the pulse, and its spectral range is a consequence of the fast switching of the transistors and modulation. Phase-shifted carrier modulation generates relatively concentrated distortion whereas other methods, such as sigma–delta modulation or predictive spectral control, could spread out the distortion if required [122, 162, 163].

Free combination of various pulses, pulse current directions, and pulse amplitudes in rapid succession

The modular pulse synthesizer technology can not only generate practically any TMS pulse, including all existing ones and a wide range of any user-defined pulses, but due to energy recovery also in rapid trains up to theta-burst and quadripulse stimulation as only little recharging is necessary. Beyond that, however, the technology can also change the pulse rapidly from pulse to pulse as needed for paired-pulse measurements with a weaker preconditioning pulse.

Figures 13 to 15 demonstrate that pulse trains can, for instance, combine pulses with different amplitude, current direction, pulse width, or entirely different shape. In the examples, the pulses are as close to each other as 50 μs to demonstrate the possible, though longer interpulse timings are unproblematic. Conventional devices, on the other hand, needed to physically reconfigure the circuit to switch, for example, from monophasic to biphasic by removing the damping resistor, which takes on the order of five to ten seconds in devices with such a feature. However, conventional device technology cannot even adjust the amplitude rapidly from pulse to pulse to a larger degree as amplitude adjustments requires charging or discharging the capacitor. The modular pulse synthesizer, however, can adjust the amplitude also through switching control as demonstrated above. The pulse shape including pulse duration and pulse direction are merely control aspects as outlined before and can be rapidly changed between pulses.

Conclusions

We presented a modular pulse synthesizer TMS device with highly flexible pulse shape control and unparalleled quality of the output pulse. Neither conventional TMS nor conventional power electronic inverter circuits could achieve such pulse-shape control as the combination of power and bandwidth overwhelms transistors while standard inverter circuits furthermore generate poor electric field output quality with large high-frequency components. MPS TMS leveraged power electronics solutions we have developed over the past decade [133–136]. The technology combines a modular circuit that breaks the requisite high power and fast switching dynamics with latest unipolar wide-bandgap semiconductors to achieve an exceptionally high power–bandwidth product. The unipolar SiC field effect transistors do not exhibit the large and slow charge-storing effects of previous power semiconductor devices in that voltage range, enabling fast switching. The implemented device can cover the range of conventional TMS devices with up to ~ 4,000 V and ~ 8,000 A, with more than 600 kHz effective switching rate and fine output granularity to cover a bandwidth of at least 60 kHz with high quality. The modular design allows easy and practically unlimited scaling of all three performance figures of voltage, current, and effective switching rate.

The MPS TMS device can generate all conventional TMS pulse shapes and pulse protocols with low distortion and future novel pulse shapes with moderate constraints, such as userdefined or mathematically optimized pulses [83]. Notably, the modular pulse synthesizer principle generates pulses through electronic control, without any intentional resistance or damping. In consequence, all pulses, including monophasic ones, are generated with energy recycling [133, 134]. Conventional TMS circuits, in contrast, can recover some of the pulse energy only for biphasic pulses. Monophasic devices, in contrast, convert the entire pulse energy into heat due to their principles of pulse shaping and therefore only reach low repetition rates. As a consequence of such energy recovery, MPS TMS can repeat all pulses, including monophasic ones, at high repetition rates.

Moreover, the technology can rapidly change any pulse features or the entire pulse shape. This rapid readjustment of pulses is in marked contrast to conventional machines, which typically could not even change the amplitude in larger steps or the current direction within rapid pulse trains or double pulses. Thus, MPS TMS can prime with one pulse amplitude or pulse shape having certain neural activation selectivity and follow up with another pulse with different amplitude and/or pulse shape having a different activation profile.

Beyond the high flexibility, the MPS TMS technology provides a number of technical advantages. In addition to the energy recovery for any pulse, we demonstrated the generation of pulses previously suggested in the literature for lower coil heating for the same stimulation strength. Moreover, the circuit principle can generate pulse shapes differentially. Thus, in contrast to conventional TMS pulse sources, the average electrical potential of the coil is approximately constant which promises to reduce the generation of capacitive artifacts in sensitive electronics, particularly neuroamplifiers, such as those for EMG, EEG, or intracranial recordings.

Acknowledgements

References

[1]. Rossini PM, Burke D, Chen R, Cohen LG, Daskalakis Z, Di Iorio R, et al. , "Non-invasive electrical and magnetic stimulation of the brain, spinal cord, roots and peripheral nerves: Basic principles and procedures for routine clinical and research application. An updated report from an I.F.C.N. Committee," Clinical Neurophysiology, vol. 126, pp. 1071–1107, 2015. [PubMed: 25797650]

[2]. Barker AT, Jalinous R, and Freeston IL, "Non-invasive magnetic stimulation of human motor cortex," The Lancet, vol. 325, pp. 1106–1107, 1985.

[3]. Ugawa Y, Rothwell JC, Day BL, Thompson PD, and Marsden CD, "Magnetic stimulation over the spinal enlargements," Journal of Neurology, Neurosurgery & Psychiatry, vol. 52, pp. 1025–1032, 1989. [PubMed: 2795071]

[4]. Nardone R, Höller Y, Taylor A, Thomschewski A, Orioli A, Frey V, et al. , "Noninvasive Spinal Cord Stimulation: Technical Aspects and Therapeutic Applications," Neuromodulation: Technology at the Neural Interface, vol. 18, pp. 580–591, 2015. [PubMed: 26245458]

[5]. Polson MJR, Barker AT, and Freeston IL, "Stimulation of nerve trunks with time-varying magnetic fields," Medical and Biological Engineering and Computing, vol. 20, pp. 243–244, 1982. [PubMed: 7098583]

[6]. Szecsi J, Goetz S, Pöllmann W, and Straube A, "Force–pain relationship in functional magnetic and electrical stimulation of subjects with paresis and preserved sensation," Clinical Neurophysiology, vol. 121, pp. 1589–1597, 2010. [PubMed: 20382558]

[7]. Goetz SM, Herzog HG, Gattinger N, and Gleich B, "Comparison of coil designs for peripheral magnetic muscle stimulation," Journal of Neural Engineering, vol. 8, p. 056007, 2011. [PubMed: 21832812]

[8]. Goetz SM and Deng Z-D, "The development and modelling of devices and paradigms for transcranial magnetic stimulation," International Review of Psychiatry, vol. 29, pp. 115–145, 2017. [PubMed: 28443696]

[9]. Gomez LJ, Goetz SM, and Peterchev AV, "Design of transcranial magnetic stimulation coils with optimal trade-off between depth, focality, and energy," Journal of Neural Engineering, vol. 15, p. 046033, 2018. [PubMed: 29855433]

[10]. Valero-Cabré A, Amengual JL, Stengel C, Pascual-Leone A, and Coubard OA, "Transcranial magnetic stimulation in basic and clinical neuroscience: A comprehensive review of fundamental principles and novel insights," Neuroscience & Biobehavioral Reviews, vol. 83, pp. 381–404, 2017. [PubMed: 29032089]

[11]. Luan S, Williams I, Nikolic K, and Constandinou TG, "Neuromodulation: present and emerging methods," Frontiers in Neuroengineering, vol. 7, 2014.

[12]. Sack AT, Kadosh RC, Schuhmann T, Moerel M, Walsh V, and Goebel R, "Optimizing Functional Accuracy of TMS in Cognitive Studies: A Comparison of Methods," Journal of Cognitive Neuroscience, vol. 21, pp. 207–221, 2009. [PubMed: 18823235]

[13]. Miniussi C, Ruzzoli M, and Walsh V, "The mechanism of transcranial magnetic stimulation in cognition," Cortex, vol. 46, pp. 128–130, 2010. [PubMed: 19356747]

[14]. Luber B and Lisanby SH, "Enhancement of human cognitive performance using transcranial magnetic stimulation (TMS)," NeuroImage, vol. 85, pp. 961–970, 2014. [PubMed: 23770409]

[15]. Levkovitz Y, Isserles M, Padberg F, Lisanby SH, Bystritsky A, Xia G, et al. , "Efficacy and safety of deep transcranial magnetic stimulation for major depression: a prospective multicenter randomized controlled trial," World Psychiatry, vol. 14, pp. 64–73, 2015. [PubMed: 25655160]

[16]. O'Reardon JP, Solvason HB, Janicak PG, Sampson S, Isenberg KE, Nahas Z, et al. , "Efficacy and Safety of Transcranial Magnetic Stimulation in the Acute Treatment of Major Depression: A Multisite Randomized Controlled Trial," Biological Psychiatry, vol. 62, pp. 1208–1216, 2007. [PubMed: 17573044]

[17]. George MS, Lisanby SH, Avery D, McDonald WM, Durkalski V, Pavlicova M, et al. , "Daily Left Prefrontal Transcranial Magnetic Stimulation Therapy for Major Depressive Disorder: A Sham-Controlled Randomized TrialMagnetic Stimulation for Major Depressive Disorder," Archives of General Psychiatry, vol. 67, pp. 507–516, 2010. [PubMed: 20439832]

[18]. Blumberger DM, Vila-Rodriguez F, Thorpe KE, Feffer K, Noda Y, Giacobbe P, et al. , "Effectiveness of theta burst versus high-frequency repetitive transcranial magnetic stimulation in patients with depression (THREE-D): a randomised non-inferiority trial," The Lancet, vol. 391, pp. 1683–1692, 2018.

[19]. Food and Drug Administration, "K122288; 510(K) Summary Brainsway Deep TMS System," ed. http://www.accessdata.fda.gov/cdrh_docs/pdf12/K122288.pdf, 2013.

[20]. Mantovani A, Simpson HB, Fallon BA, Rossi S, and Lisanby SH, "Randomized sham-controlled trial of repetitive transcranial magnetic stimulation in treatment-resistant obsessive–compulsive disorder," International Journal of Neuropsychopharmacology, vol. 13, pp. 217–227, 2010. [PubMed: 19691873]

[21]. Lipton RB, Dodick DW, Silberstein SD, Saper JR, Aurora SK, Pearlman SH, et al. , "Single-pulse transcranial magnetic stimulation for acute treatment of migraine with aura: a randomised, double-blind, parallel-group, sham-controlled trial," The Lancet Neurology, vol. 9, pp. 373–380, 2010. [PubMed: 20206581]

[22]. Picht T, Schmidt S, Brandt S, Frey D, Hannula H, Neuvonen T, et al. , "Preoperative Functional Mapping for Rolandic Brain Tumor Surgery: Comparison of Navigated Transcranial Magnetic Stimulation to Direct Cortical Stimulation," Neurosurgery, vol. 69, pp. 581–589, 2011. [PubMed: 21430587]

[23]. Takahashi S and Picht T, "Comparison of Navigated Transcranial Magnetic Stimulation to Direct Electrical Stimulation for Mapping the Motor Cortex Prior to Brain Tumor Resection," in Tumors of the Central Nervous System, Volume 12: Molecular Mechanisms, Children's Cancer, Treatments, and Radiosurgery, Hayat MA, Ed., ed Dordrecht: Springer Netherlands, 2014, pp. 261–276.

[24]. Zangen A, Moshe H, Martinez D, Barnea-Ygael N, Vapnik T, Bystritsky A, et al. , "Repetitive transcranial magnetic stimulation for smoking cessation: a pivotal multicenter double-blind randomized controlled trial," World Psychiatry, vol. 20, pp. 397–404, 2021. [PubMed: 34505368]

[25]. Eldaief MC, Press DZ, and Pascual-Leone A, "Transcranial magnetic stimulation in neurology: A review of established and prospective applications," Neurology Clinical Practice, vol. 3, pp. 519–526, 2013. [PubMed: 24353923]

[26]. Marzouk T, Winkelbeiner S, Azizi H, Malhotra AK, and Homan P, "Transcranial Magnetic Stimulation for Positive Symptoms in Schizophrenia: A Systematic Review," Neuropsychobiology, vol. 79, pp. 384–396, 2020. [PubMed: 31505508]

[27]. Fisicaro F, Lanza G, Grasso AA, Pennisi G, Bella R, Paulus W, et al. , "Repetitive transcranial magnetic stimulation in stroke rehabilitation: review of the current evidence and pitfalls," Therapeutic Advances in Neurological Disorders, vol. 12, p. 1756286419878317, 2019. [PubMed: 31598137]

[28]. Peterchev AV, Deng ZD, and Goetz SM, "Advances in Transcranial Magnetic Stimulation Technology," in Brain Stimulation, ed: John Wiley & Sons, 2015, pp. 165–189.

[29]. Thielscher A and Kammer T, "Electric field properties of two commercial figure-8 coils in TMS: calculation of focality and efficiency," Clinical Neurophysiology, vol. 115, pp. 1697–1708, 2004. [PubMed: 15203072]

[30]. Deng Z-D, Lisanby SH, and Peterchev AV, "Electric field depth–focality tradeoff in transcranial magnetic stimulation: Simulation comparison of 50 coil designs," Brain Stimulation, vol. 6, pp. 1–13, 2013. [PubMed: 22483681]

[31]. Karabanov A, Ziemann U, Hamada M, George MS, Quartarone A, Classen J, et al. , "Consensus Paper: Probing Homeostatic Plasticity of Human Cortex With Non-invasive Transcranial Brain Stimulation," Brain Stimulation, vol. 8, pp. 993–1006, 2015. [PubMed: 26598772]

[32]. Stokes MG, Barker AT, Dervinis M, Verbruggen F, Maizey L, Adams RC, et al. , "Biophysical determinants of transcranial magnetic stimulation: effects of excitability and depth of targeted area," Journal of Neurophysiology, vol. 109, pp. 437–444, 2012. [PubMed: 23114213]

[33]. Aberra AS, Wang B, Grill WM, and Peterchev AV, "Simulation of transcranial magnetic stimulation in head model with morphologically-realistic cortical neurons," Brain Stimulation, vol. 13, pp. 175–189, 2020. [PubMed: 31611014]

[34]. Lontis ER, Voigt M, and Struijk JJ, "Focality Assessment in Transcranial Magnetic Stimulation With Double and Cone Coils," Journal of Clinical Neurophysiology, vol. 23, pp. 463–472, 2006.

[35]. Bargmann CI and Newsome WT, "The Brain Research Through Advancing Innovative Neurotechnologies (BRAIN) Initiative and Neurology," JAMA Neurology, vol. 71, pp. 675–676, 2014. [PubMed: 24711071]

[36]. Mosier EM, Wolfson M, Ross E, Harris J, Weber D, and Ludwig KA, "Chapter 5 - The Brain Initiative—Implications for a Revolutionary Change in Clinical Medicine via Neuromodulation Technology," in Neuromodulation (Second Edition), Krames ES, Peckham PH, and Rezai AR, Eds., ed: Academic Press, 2018, pp. 55–68.

[37]. Di Lazzaro V, Rothwell J, and Capogna M, "Noninvasive Stimulation of the Human Brain: Activation of Multiple Cortical Circuits," The Neuroscientist, vol. 24, pp. 246–260, 2017. [PubMed: 28659070]

[38]. Strigaro G, Hamada M, C. R, and Rothwell JC, "Variability in response to 1 Hz repetitive TMS," Brain Stimulation: Basic, Translational, and Clinical Research in Neuromodulation, vol. 8, pp. 383–384, 2015.

[39]. Maeda F, Keenan JP, Tormos JM, Topka H, and Pascual-Leone A, "Interindividual variability of the modulatory effects of repetitive transcranial magnetic stimulation on cortical excitability," Experimental Brain Research, vol. 133, pp. 425–430, 2000. [PubMed: 10985677]

[40]. Guerra A, López-Alonso V, Cheeran B, and Suppa A, "Variability in non-invasive brain stimulation studies: Reasons and results," Neuroscience Letters, 2017.

[41]. Huang Y-Z, Lu M-K, Antal A, Classen J, Nitsche M, Ziemann U, et al. , "Plasticity induced by non-invasive transcranial brain stimulation: A position paper," Clinical Neurophysiology, vol. 128, pp. 2318–2329, 2017. [PubMed: 29040922]

[42]. Kar SK, "Predictors of Response to Repetitive Transcranial Magnetic Stimulation in Depression: A Review of Recent Updates," Clinical Psychopharmacology and Neuroscience, vol. 17, pp. 25–33, 2019. [PubMed: 30690937]

[43]. Goetz SM, Luber B, Lisanby SH, Murphy DL, Kozyrkov IC, Grill WM, et al. , "Enhancement of Neuromodulation with Novel Pulse Shapes Generated by Controllable Pulse Parameter Transcranial Magnetic Stimulation," Brain Stimul, vol. 9, pp. 39–47, 2016. [PubMed: 26460199]

[44]. Rothwell J and Hannah R, "Effects of pulse width on responses to single, double and repetitive TMS of motor cortex," Brain Stimulation, vol. 12, p. 588, 2019.

[45]. D'Ostilio K, Goetz SM, Ciocca M, Chieffo R, Chen J-CA, Peterchev AV, et al. , "Effect of coil orientation on strength-duration time constant with controllable pulse parameter transcranial magnetic stimulation," Clinical Neurophysiology, vol. 125 (Suppl. 1), p. S123, 2014.

[46]. Casula EP, Rocchi L, Hannah R, and Rothwell JC, "Effects of pulse width, waveform and current direction in the cortex: A combined cTMS-EEG study," Brain Stimulation, vol. 11, pp. 1063–1070, 2018. [PubMed: 29709505]

[47]. Sommer M, Ciocca M, Chieffo R, Hammond P, Neef A, Paulus W, et al. , "TMS of primary motor cortex with a biphasic pulse activates two independent sets of excitable neurones," Brain Stimulation, vol. 11, pp. 558–565, 2018. [PubMed: 29352669]

[48]. Hannah R and Rothwell JC, "Pulse Duration as Well as Current Direction Determines the Specificity of Transcranial Magnetic Stimulation of Motor Cortex during Contraction," Brain Stimulation, vol. 10, pp. 106–115, 2017. [PubMed: 28029595]

[49]. Shirota Y, Dhaka S, Paulus W, and Sommer M, "Current direction-dependent modulation of human hand motor function by intermittent theta burst stimulation (iTBS)," Neuroscience Letters, vol. 650, pp. 109–113, 2017. [PubMed: 28435045]

[50]. Sommer M, Alfaro A, Rummel M, Speck S, Lang N, Tings T, et al. , "Half sine, monophasic and biphasic transcranial magnetic stimulation of the human motor cortex," Clinical Neurophysiology, vol. 117, pp. 838–844, 2006. [PubMed: 16495145]

[51]. Sommer M, Norden C, Schmack L, Rothkegel H, Lang N, and Paulus W, "Opposite Optimal Current Flow Directions for Induction of Neuroplasticity and Excitation Threshold in the Human Motor Cortex," Brain Stimulation, vol. 6, pp. 363–370, 2013. [PubMed: 22885142]

[52]. Kammer T, Beck S, Erb M, and Grodd W, "The influence of current direction on phosphene thresholds evoked by transcranial magnetic stimulation," Clinical Neurophysiology, vol. 112, pp. 2015–2021, 2001. [PubMed: 11682339]

[53]. Kammer T, Beck S, Thielscher A, Laubis-Herrmann U, and Topka H, "Motor thresholds in humans: a transcranial magnetic stimulation study comparing different pulse waveforms, current directions and stimulator types," Clinical Neurophysiology, vol. 112, pp. 250–258, 2001. [PubMed: 11165526]

[54]. Kammer T, Vorwerg M, and Herrnberger B, "Anisotropy in the visual cortex investigated by neuronavigated transcranial magnetic stimulation," NeuroImage, vol. 36, pp. 313–321, 2007. [PubMed: 17442592]

[55]. Lazzaro V, Oliviero A, Mazzone P, Insola A, Pilato F, Saturno E, et al. , "Comparison of descending volleys evoked by monophasic and biphasic magnetic stimulation of the motor cortex in conscious humans," Experimental Brain Research, vol. 141, pp. 121–127, 2001. [PubMed: 11685416]

[56]. Spampinato D, "Dissecting two distinct interneuronal networks in M1 with transcranial magnetic stimulation," Experimental Brain Research, 2020.

[57]. Hannah R, Rocchi L, Tremblay S, Wilson E, and Rothwell JC, "Pulse width biases the balance of excitation and inhibition recruited by transcranial magnetic stimulation," Brain Stimulation: Basic, Translational, and Clinical Research in Neuromodulation, vol. 13, pp. 536–538, 2020.

[58]. Davila-Pérez P, Jannati A, Fried PJ, Cudeiro Mazaira J, and Pascual-Leone A, "The Effects of Waveform and Current Direction on the Efficacy and Test–Retest Reliability of Transcranial Magnetic Stimulation," Neuroscience, vol. 393, pp. 97–109, 2018. [PubMed: 30300705]

[59]. Halawa I, Shirota Y, Neef A, Sommer M, and Paulus W, "Neuronal tuning: Selective targeting of neuronal populations via manipulation of pulse width and directionality," Brain Stimulation, vol. 12, p. 399, 2019.

[60]. Halawa I, Shirota Y, Neef A, Sommer M, and Paulus W, "Longer cTMS pulse width switches 1 Hz inhibitory motor cortex rTMS aftereffects to excitation," Brain Stimulation: Basic, Translational, and Clinical Research in Neuromodulation, vol. 12, p. 589, 2019.

[61]. Sommer M, Lang N, Tergau F, and Paulus W, "Neuronal tissue polarization induced by repetitive transcranial magnetic stimulation?," Neuroreport, vol. 13, pp. 809–11, 2002. [PubMed: 11997692]

[62]. Antal A, Kincses TZ, Nitsche MA, Bartfai O, Demmer I, Sommer M, et al. , "Pulse configuration-dependent effects of repetitive transcranial magnetic stimulation on visual perception," Neuroreport, vol. 13, pp. 2229–33, 2002. [PubMed: 12488802]

[63]. Tings T, Lang N, Tergau F, Paulus W, and Sommer M, "Orientation-specific fast rTMS maximizes corticospinal inhibition and facilitation," Exp Brain Res, vol. 164, pp. 323–33, 2005. [PubMed: 15868175]

[64]. Nakamura K, Groiss SJ, Hamada M, Enomoto H, Kadowaki S, Abe M, et al. , "Variability in Response to Quadripulse Stimulation of the Motor Cortex," Brain Stimulation, vol. 9, pp. 859–866, 2016. [PubMed: 27692928]

[65]. Taylor JL and Loo CK, "Stimulus waveform influences the efficacy of repetitive transcranial magnetic stimulation," Journal of Affective Disorders, vol. 97, pp. 271–276, 2007. [PubMed: 16887197]

[66]. Hosono Y, Urushihara R, Harada M, Morita N, Murase N, Kunikane Y, et al. , "Comparison of monophasic versus biphasic stimulation in rTMS over premotor cortex: SEP and SPECT studies," Clinical Neurophysiology, vol. 119, pp. 2538–2545, 2008. [PubMed: 18835216]

[67]. McRobbie D, "Design and instrumentation of a magnetic nerve stimulator," Journal of Physics E: Scientific Instruments, vol. 18, p. 74, 1985.

[68]. Schmid M, Weyh T, and Meyer B-U, "Entwicklung, Optimierung und Erprobung neuer Geräte für die magnetomotorische Stimulation von Nervenfasern / Development, Optimization, and Testing of New Devices for Magnetomotive Fibre Stimulation," Biomedizinische Technik / Biomedical Engineering, vol. 38, pp. 317–324, 1993. [PubMed: 8123772]

[69]. Huang Y-Z, Edwards MJ, Rounis E, Bhatia KP, and Rothwell JC, "Theta Burst Stimulation of the Human Motor Cortex," Neuron, vol. 45, pp. 201–206, 2005. [PubMed: 15664172]

[70]. Jung NH, Gleich B, Gattinger N, Hoess C, Haug C, Siebner HR, et al. , "Quadri-Pulse Theta Burst Stimulation using Ultra-High Frequency Bursts – A New Protocol to Induce Changes in Cortico-Spinal Excitability in Human Motor Cortex," PLOS ONE, vol. 11, p. e0168410, 2016. [PubMed: 27977758]

[71]. Hamada M and Ugawa Y, "Quadripulse stimulation – A new patterned rTMS," Restorative Neurology and Neuroscience, vol. 28, pp. 419–424, 2010. [PubMed: 20714066]

[72]. Simeoni S, Hannah R, Sato D, Kawakami M, Rothwell J, Simeoni S, et al. , "Effects of Quadripulse Stimulation on Human Motor Cortex Excitability: A Replication Study," Brain Stimulation, vol. 9, pp. 148–150, 2016. [PubMed: 26596527]

[73]. D'Ostilio K, Goetz SM, Hannah R, Ciocca M, Chieffo R, Chen J-CA, et al. , "Effect of coil orientation on strength–duration time constant and I-wave activation with controllable pulse parameter transcranial magnetic stimulation," Clinical Neurophysiology, vol. 127, pp. 675–683, 2016. [PubMed: 26077634]

[74]. Sommer M, D'Ostilio K, Cioccia M, Hannah R, Hammond P, Goetz S, et al. , "TMS can selectively activate and condition two different sets of excitatory synaptic inputs to corticospinal neurons in humans," SFN Society for Neuroscience, p. 542, 2014.

[75]. Peterchev AV, Luber B, Westin GG, and Lisanby SH, "Pulse Width Affects Scalp Sensation of Transcranial Magnetic Stimulation," Brain Stimulation, vol. 10, pp. 99–105, 2017. [PubMed: 28029593]

[76]. Goetz SM, Murphy DLK, and Peterchev AV, "Transcranial Magnetic Stimulation Device With Reduced Acoustic Noise," IEEE Magnetics Letters, vol. 5, pp. 1–4, 2014.

[77]. Goetz SM, Lisanby SH, Murphy DLK, Price RJ, O'Grady G, and Peterchev AV, "Impulse Noise of Transcranial Magnetic Stimulation: Measurement, Safety, and Auditory Neuromodulation," Brain Stimulation: Basic, Translational, and Clinical Research in Neuromodulation, vol. 8, pp. 161–163, 2015.

[78]. Peterchev AV, Murphy DLK, and Goetz SM, "Quiet transcranial magnetic stimulation: Status and future directions," in 2015 37th Annual International Conference of the IEEE Engineering in Medicine and Biology Society (EMBC), 2015, pp. 226–229.

[79]. Zeng Z, Koponen LM, Hamdan R, Li Z, Goetz SM, and Peterchev AV, "Modular multilevel TMS device with wide output range and ultrabrief pulse capability for sound reduction," bioRxiv, p. 2021.09.08.459501, 2021.

[80]. Koponen LM, Goetz SM, and Peterchev AV, "Double-Containment Coil With Enhanced Winding Mounting for Transcranial Magnetic Stimulation With Reduced Acoustic Noise," IEEE Transactions on Biomedical Engineering, vol. 68, pp. 2233–2240, 2021. [PubMed: 33378258]

[81]. Counter SA, "Auditory brainstem and cortical responses following extensive transcranial magnetic stimulation," Journal of the Neurological Sciences, vol. 124, pp. 163–170, 1994. [PubMed: 7964867]

[82]. Clapp WC, Hamm JP, Kirk IJ, and Teyler TJ, "Translating Long-Term Potentiation from Animals to Humans: A Novel Method for Noninvasive Assessment of Cortical Plasticity," Biological Psychiatry, vol. 71, pp. 496–502, 2012. [PubMed: 21974785]

[83]. Goetz SM, Truong CN, Gerhofer MG, Peterchev AV, Herzog H-G, and Weyh T, "Analysis and Optimization of Pulse Dynamics for Magnetic Stimulation," PLoS ONE, vol. 8, p. e55771, 2013. [PubMed: 23469168]

[84]. Goetz SM, Truong NC, Gerhofer MG, Peterchev AV, Herzog HG, and Weyh T, "Optimization of magnetic neurostimulation waveforms for minimum power loss," IEEE Proc. Engin. Med. Biol, vol. 34, pp. 4652–4655, 2012.

[85]. Rossi S, Hallett M, Rossini PM, and Pascual-Leone A, "Safety, ethical considerations, and application guidelines for the use of transcranial magnetic stimulation in clinical practice and research," Clinical Neurophysiology, vol. 120, pp. 2008–2039, 2009. [PubMed: 19833552]

[86]. UL 60601–1 Medical Electrical Equipment, Part 1: General Requirements for Safety, UL, 2012.

[87]. Peterchev AV, Goetz SM, Westin GG, Luber B, and Lisanby SH, "Pulse width dependence of motor threshold and input–output curve characterized with controllable pulse parameter transcranial magnetic stimulation," Clinical Neurophysiology, vol. 124, pp. 1364–1372, 2013. [PubMed: 23434439]

[88]. Barker AT, Garnham CW, and Freeston IL, "Magnetic nerve stimulation: the effect of waveform on efficiency, determination of neural membrane time constants and the measurement of stimulator output," Electroencephalogr Clin Neurophysiol Supplement, vol. 43, pp. 227–37, 1991.

[89]. Jalinous R, "Principles of magnetic stimulator design," in Handbook of Transcranial Magnetic Stimulation, Pascual A, Davey NJ, Rothwell JC, Wassermann EM, and Puri BK, Eds., ed London: Arnold, 2002.

[90]. Rothkegel H, Sommer M, Paulus W, and Lang N, "Impact of pulse duration in single pulse TMS," Clinical Neurophysiology, vol. 121, pp. 1915–1921, 2010. [PubMed: 20444645]

[91]. Peterchev AV, Deng Z-D, and Goetz SM, "Advances in transcranial magnetic stimulation technology," in Brain Stimulation: Methodologies and Interventions, Reti IM, Ed., ed Hoboken, NJ: John Wiley & Sons, 2015.

[92]. Claus D, Murray NMF, Spitzer A, and Flügel D, "The influence of stimulus type on the magnetic excitation of nerve structures," Electroencephalography and Clinical Neurophysiology, vol. 75, pp. 342–349, 1990. [PubMed: 1691083]

[93]. Jalinous R, "Technical and Practival Aspects of Magnetic Nerve Stimulation," Journal of Clinical Neurophysiology, vol. 8, pp. 10–25, 1991. [PubMed: 2019644]

[94]. Cadwell J, "Optimizing magnetic stimulator design," Electroencephalography and clinical neurophysiology Supplement, vol. 43, pp. 238–248, 1991.

[95]. Wessel MJ, Draaisma LR, Morishita T, and Hummel FC, "The Effects of Stimulator, Waveform, and Current Direction on Intracortical Inhibition and Facilitation: A TMS Comparison Study," Frontiers in Neuroscience, vol. 13, 2019.

[96]. Peterchev AV, D'Ostilio K, Rothwell JC, and Murphy DL, "Controllable pulse parameter transcranial magnetic stimulator with enhanced circuit topology and pulse shaping," Journal of Neural Engineering, vol. 11, p. 056023, 2014. [PubMed: 25242286]

[97]. Barker AT, Garnham CW, and Freeston IL, "Magnetic nerve stimulation: the effect of waveform on efficiency, determination of neural membrane time constants and the measurement of stimulator output," Electroencephalography and clinical neurophysiology Supplement, vol. 43, pp. 227–237, 1991.

[98]. Lang N, Harms J, Weyh T, Lemon RN, Paulus W, Rothwell JC, et al. , "Stimulus intensity and coil characteristics influence the efficacy of rTMS to suppress cortical excitability," Clinical Neurophysiology, vol. 117, pp. 2292–2301, 2006. [PubMed: 16920022]

[99]. Peterchev AV, Murphy DL, and Lisanby SH, "Repetitive transcranial magnetic stimulator with controllable pulse parameters," Journal of Neural Engineering, vol. 8, p. 036016, 2011. [PubMed: 21540487]

[100]. Peterchev AV, Jalinous R, and Lisanby SH, "A Transcranial Magnetic Stimulator Inducing Near-Rectangular Pulses With Controllable Pulse Width (cTMS)," IEEE Transactions on Biomedical Engineering, vol. 55, pp. 257–266, 2008. [PubMed: 18232369]

[101]. Moritz M, Schmitt F, Schweighofer P, and Havel P, "Magnetic Stimulation Device," Siemens AG, Patent, US 6,450,940; EP 0 996 485; European Patent Office, U.S. Patent and Trademark Office 2002.

[102]. Gattinger N, Mossnang G, and Gleich B, "flexTMS – A Novel Repetitive Transcranial Magnetic Stimulation Device With Freely Programmable Stimulus Currents," Biomedical Engineering, IEEE Transactions on, vol. 59, pp. 1962–1970, 2012.

[103]. Koponen LM, Nieminen JO, Mutanen TP, Stenroos M, and Ilmoniemi RJ, "Coil optimisation for transcranial magnetic stimulation in realistic head geometry," Brain Stimulation, vol. 10, pp. 795–805, 2017. [PubMed: 28461068]

[104]. Peterchev AV, "Circuit topology comparison and design analysis for controllable pulse parameter transcranial magnetic stimulators," in Neural Engineering (NER), 2011 5th International IEEE/EMBS Conference on, 2011, pp. 646–649.

[105]. Boyden ES, Kim M, Abram G, and Henninger M, "Portable modular transcranial magnetic stimulation device," Massachusetts Institute of Technology, Patent, US 2009/0018384 A1, US 12/117,896, U.S. Patent and Trademark Office 2009.

[106]. Talebinejad M and Chan ADC, "Circuit and method for use in transranial magnetic stimulation," US 9,504,846 B2, US 14/442,543, U.S. Patent and Trademark Office 2016.

[107]. Roth Y, Zangen A, Chudnovsky V, Safra N, and Hazani D, "Systems and Methods for Controlling Electric Field Pulse Parameters Using Transcranial Magnetic Stimulation," Yeda Research & Development Co. Ltd. at the Weizmann Institute of Science, Patent, US 9,180,305; EP 2 376 178 B1, US 2010/0152522, European Patent Office, U.S. Patent and Trademark Office 2015.

[108]. Goetz SM and Weyh T, "Vorrichtung zur Nervenreizung mit Magnetfeldimpulsen," Technische Universität München, Patent, DE 10 2009 023 855 B4, DE 10 2009 023 855.7, Deutsches Patent- und Markenamt (DPMA) 2009.

[109]. Corthout E, Barker A, and Cowey A, "Transcranial magnetic stimulation. Which part of the current waveform causes the stimulation?," Experimental Brain Research, vol. 141, pp. 128–132, 2001. [PubMed: 11685417]

[110]. Riehl M, "TMS stimulator design," in Oxford Handbook of Transcranial Stimulation, Wassermann EM, Epstein CM, Ziemann U, Walsh V, Paus T, and Lisanby SH, Eds., ed Oxford: Oxford University Press, 2008, pp. 13–23.

[111]. Epstein CM, "A six-pound battery-powered portable transcranial magnetic stimulator," Brain Stimulation, vol. 1, pp. 128–130, 2008. [PubMed: 20633379]

[112]. Machida S, Ito K, and Yamashita Y, "Approaching the limit of switching loss reduction in Si-IGBTs," in Power Semiconductor Devices & IC's (ISPSD), 2014 IEEE 26th International Symposium on, 2014, pp. 107–110.

[113]. Qian J, Khan A, and Batarseh I, "Turn-off switching loss model and analysis of IGBT under different switching operation modes," in Industrial Electronics, Control, and Instrumentation, 1995., Proceedings of the 1995 IEEE IECON 21st International Conference on, 1995, pp. 240–245 vol.1.

[114]. Oliveira AC, Jacobina CB, and Lima AMN, "Improved Dead-Time Compensation for Sinusoidal PWM Inverters Operating at High Switching Frequencies," Industrial Electronics, IEEE Transactions on, vol. 54, pp. 2295–2304, 2007.

[115]. Emrich D, Fischer A, Altenhöfer C, Weyh T, Helling F, Goetz S, et al. , "Muscle force development after low-frequency magnetic burst stimulation in dogs," Muscle & Nerve, vol. 46, pp. 951–953, 2012. [PubMed: 23225386]

[116]. Hermsen AM, Haag A, Duddek C, Balkenhol K, Bugiel H, Bauer S, et al. , "Test–retest reliability of single and paired pulse transcranial magnetic stimulation parameters in healthy subjects," Journal of the Neurological Sciences, vol. 362, pp. 209–216, 2016. [PubMed: 26944150]

[117]. Ferreri F, Pasqualetti P, Määttä S, Ponzo D, Ferrarelli F, Tononi G, et al. , "Human brain connectivity during single and paired pulse transcranial magnetic stimulation," NeuroImage, vol. 54, pp. 90–102, 2011. [PubMed: 20682352]

[118]. Boroojerdi B, Kopylev L, Battaglia F, Facchini S, Ziemann U, Muellbacher W, et al. , "Reproducibility of intracortical inhibition and facilitation using the paired-pulse paradigm," Muscle & Nerve, vol. 23, pp. 1594–1597, 2000. [PubMed: 11003798]

[119]. Reis J, Swayne OB, Vandermeeren Y, Camus M, Dimyan MA, Harris-Love M, et al. , "Contribution of transcranial magnetic stimulation to the understanding of cortical mechanisms involved in motor control," The Journal of Physiology, vol. 586, pp. 325–351, 2008. [PubMed: 17974592]

[120]. Schweighofer P, Moritz M, and Schmitt F, "Magnetic stimulation device," Siemens AG, Patent, US 6,123,658; EP 0 958 844, US 09/313,559, European Patent Office, U.S. Patent and Trademark Office 2000.

[121]. Emadi A, Young Joo L, and Rajashekara K, "Power Electronics and Motor Drives in Electric, Hybrid Electric, and Plug-In Hybrid Electric Vehicles," Industrial Electronics, IEEE Transactions on, vol. 55, pp. 2237–2245, 2008.

[122]. Goetz S and Korte C, "Spectral synthesis of switching distortion in automotive drive inverters," in 2016 18th European Conference on Power Electronics and Applications (EPE'16 ECCE Europe), 2016, pp. 1–10.

[123]. Polson MJR, "Magnetic stimulator with increased energy efficiency " Magstim Co., Patent, GB 2 298 370, UK Intellectual Property Office 1996.

[124]. Polson MJR, "Magnetic stimulator for neuro-muscular tissue " Magstim Co., Patent, US 5,766,124, U.S. Patent and Trademark Office 1998.

[125]. Mazac K, "Verfahren und Vorrichtung zur Anwendung von elektromagnetischen Feldern (EMF) in therapeutischer Praxis," DE 10 2010 009 743, DE 10 2010 009 743, Deutsches Patent- und Markenamt (DPMA) 2010.

[126]. Perreault DJ and Mogren S, "Magnetic stimulator power and control circuit," R. B. Carr Engineering, Patent, US 6,551,233 B2, US 09/924,907, U.S. Patent and Trademark Office 2003.

[127]. Mogyoros I, Kiernan MC, Burke D, and Bostock H, "Strength-duration properties of sensory and motor axons in amyotrophic lateral sclerosis," Brain, vol. 121, pp. 851–859, 1998. [PubMed: 9619189]

[128]. Chen P, Wu P, Wan X, Wang Q, Xu C, Yang M, et al. , "Ultrasound-driven electrical stimulation of peripheral nerves based on implantable piezoelectric thin film nanogenerators," Nano Energy, vol. 86, p. 106123, 2021.

[129]. Moffitt MA, Mcintyre CC, and Grill WM, "Prediction of myelinated nerve fiber stimulation thresholds: limitations of linear models," IEEE Transactions on Biomedical Engineering, vol. 51, pp. 229–236, 2004. [PubMed: 14765695]

[130]. Motz H and Rattay F, "A study of the application of the Hodgkin-Huxley and the Frankenhaeuser-Huxley model for electrostimulation of the acoustic nerve," Neuroscience, vol. 18, pp. 699–712, 1986. [PubMed: 3748378]

[131]. Izhikevich EM, "Resonate-and-fire neurons," Neural Networks, vol. 14, pp. 883–894, 2001. [PubMed: 11665779]

[132]. McIntyre CC, Richardson AG, and Grill WM, "Modeling the Excitability of Mammalian Nerve Fibers: Influence of Afterpotentials on the Recovery Cycle," Journal of Neurophysiology, vol. 87, pp. 995–1006, 2002. [PubMed: 11826063]

[133]. Goetz SM, Pfaeffl M, Huber J, Singer M, Marquardt R, and Weyh T, "Circuit topology and control principle for a first magnetic stimulator with fully controllable waveform," Proc. IEEE Eng. Med. Biol. EMBC, vol. 34, pp. 4700–4703, 2012.

[134]. Goetz SM, Singer M, Huber J, Pfaeffl M, Marquardt R, and Weyh T, "Magnetic Stimulation with Arbitrary Waveform Shapes," in IFMBE Proceedings, Medical Physics and Biomedical Engineering, Beijing, 2013, pp. 2244–2247 doi: 10.1109/EMBC.2012.6347016.

[135]. Goetz SM, Peterchev AV, and Weyh T, "Modular Multilevel Converter With Series and Parallel Module Connectivity: Topology and Control," Power Electronics, IEEE Transactions on, vol. 30, pp. 203–215, 2015.

[136]. Goetz S and Weyh T, "Magnetic stimulation having a freely selectable pulse shape," Technische Universitaet Muenchen, Patent, US 9,999,780; DE 10 2010 004 307 B4; EP 2 523 726, D. P.-u. M. D. U.S. Patent and Trademark Office, European Patent Office, 2010.

[137]. Goetz S, Weyh T, and Herzog H-G, "Circuit topologies and methods for magnetic stimulation," TU Muenchen, Patent, DE 10 2012 101 921 B4, Deutsches Patent- und Markenamt (DPMA) 2012.

[138]. Goetz SM, "Electronic circuit for magnetic neurostimulation and associated control " DE 10 2017 113 581, Deutsches Patent- und Markenamt (DPMA) 2017.

[139]. Goetz SM, "Electronic Circuit for Magnetic Neurostimulation and Associated Control," US 2018/0361 168, U.S. Patent and Trademark Office 2018.

[140]. Zeng Z, Koponen LM, Hamdan R, Li Z, Goetz SM, and Peterchev AV, "Modular multilevel TMS device with wide output range and ultrabrief pulse capability for sound reduction," Journal of Neural Engineering, vol. 19, p. 026008, 2022.

[141]. Iwamuro N and Laska T, "IGBT History, State-of-the-Art, and Future Prospects," IEEE Transactions on Electron Devices, vol. 64, pp. 741–752, 2017.

[142]. Li HH, Trivedi M, and Shenai K, "Dynamics of IGBT performance in hard- and soft-switching converters," in IAS '95. Conference Record of the 1995 IEEE Industry Applications Conference Thirtieth IAS Annual Meeting, 1995, pp. 1006–1009 vol.2.

[143]. Saito W, Ono S, and Yamashita H, "Influence of carrier lifetime control process in superjunction MOSFET characteristics," in 2014 IEEE 26th International Symposium on Power Semiconductor Devices & IC's (ISPSD), 2014, pp. 87–90.

[144]. Jahdi S, Alatise O, Bonyadi R, Alexakis P, Fisher CA, Gonzalez JAO, et al. , "An Analysis of the Switching Performance and Robustness of Power MOSFETs Body Diodes: A Technology Evaluation," IEEE Transactions on Power Electronics, vol. 30, pp. 2383–2394, 2015.

[145]. Udrea F, Deboy G, and Fujihira T, "Superjunction Power Devices, History, Development, and Future Prospects," IEEE Transactions on Electron Devices, vol. 64, pp. 713–727, 2017.

[146]. Fang J, Blaabjerg F, Liu S, and Goetz S, "A Review of Multilevel Converters with Parallel Connectivity," IEEE Transactions on Power Electronics, vol. 36, pp. 12468–12489, 2021.

[147]. Freche D, Naim-Feil J, Peled A, Levit-Binnun N, and Moses E, "A quantitative physical model of the TMS-induced discharge artifacts in EEG," PLOS Computational Biology, vol. 14, p. e1006177, 2018. [PubMed: 30016315]

[148]. Goetz SM, Li Z, Liang X, Zhang C, Lukic SM, and Peterchev AV, "Control of Modular Multilevel Converter With Parallel Connectivity—Application to Battery Systems," IEEE Transactions on Power Electronics, vol. 32, pp. 8381–8392, 2017.

[149]. Li Z, Lizana R, Peterchev AV, and Goetz SM, "Distributed balancing control for modular multilevel series/parallel converter with capability of sensorless operation," IEEE Energ Conv Con and Exp (ECCE), pp. 1787–1793, 2017.

[150]. Li Z, Lizana R, Sha S, Yu Z, Peterchev AV, and Goetz S, "Module Implementation and Modulation Strategy for Sensorless Balancing in Modular Multilevel Converters," IEEE Transactions on Power Electronics, vol. 34, pp. 8405–8416, 2018.

[151]. Li Z, Lizana R, Yu Z, Sha S, Peterchev AV, and Goetz S, "A Modular Multilevel Series/Parallel Converter for Wide Frequency Range Operation," IEEE Transactions on Power Electronics, vol. 34, pp. 9854–9865, 2019.

[152]. Li Z, Motwani JK, Zeng Z, Lukic S, Peterchev AV, and Goetz S, "A Reduced Series/Parallel Module for Cascade Multilevel Static Compensators Supporting Sensorless Balancing," IEEE Transactions on Industrial Electronics, vol. 68, no. 1, pp. 15–24, 2021.

[153]. Dekka A, Wu B, Yaramasu V, Fuentes RL, and Zargari NR, "Model Predictive Control of High-Power Modular Multilevel Converters—An Overview," IEEE Journal of Emerging and Selected Topics in Power Electronics, vol. 7, pp. 168–183, 2019.

[154]. Jiang H and Venkataramanan G, "Delta-sigma modulators for modular multilevel converters," in 2017 IEEE Energy Conversion Congress and Exposition (ECCE), 2017, pp. 1473–1478.

[155]. De Simone D, Tricoli P, D'Arco S, and Piegari L, "Windowed PWM: A Configurable Modulation Scheme for Modular Multilevel Converter-Based Traction Drives," IEEE Transactions on Power Electronics, vol. 35, pp. 9727–9736, 2020.

[156]. Montero-Robina P, Marquez A, Dahidah MSA, Vazquez S, Leon JI, Konstantinou G, et al. , "Feedforward Modulation Technique for More Accurate Operation of Modular Multilevel Converters," IEEE Transactions on Power Electronics, vol. 37, pp. 1700–1710, 2022.

[157]. Li Z, Lizana R, Peterchev AV, and Goetz SM, "Predictive control of modular multilevel series/ parallel converter for battery systems," IEEE Energ. Conv. Con. Exp. (ECCE), pp. 5685–5691, 2017.

[158]. Wang C, Li Z, Murphy DLK, Li Z, Peterchev AV, and Goetz SM, "Photovoltaic multilevel inverter with distributed maximum power point tracking and dynamic circuit reconfiguration," IEEE Int. Fut. Ener. Elec. Con. (IFEEC ECCE Asia), vol. 3, pp. 1520–1525, 2017.

[159]. Tashakor N, Li Z, and Goetz SM, "A Generic Scheduling Algorithm for Low-Frequency Switching in Modular Multilevel Converters With Parallel Functionality," IEEE Transactions on Power Electronics, vol. 36, pp. 2852–2863, 2021.

[160]. Goetz SM, Weyh T, and Herzog H, "Analysis of a magnetic stimulation system: Magnetic harmonic multi-cycle stimulation (MHMS)," in 2009 International Conference on Biomedical and Pharmaceutical Engineering, 2009, pp. 1–6.

[161]. Goetz SM, Murphy DLK, and Peterchev AV, "Magnetic neurostimulation with reduced acoustic emission," US 10,471,272, U.S. Patent and Trademark Office 2019.

[162]. Paramesh J and von Jouanne A, "Use of sigma-delta modulation to control EMI from switch-mode power supplies," Industrial Electronics, IEEE Transactions on, vol. 48, pp. 111–117, 2001.

[163]. Korte C, Luetje T, Tashakor N, and Goetz S, "Synchronous Multistep Predictive Spectral Control of the Switching Distortion in DC–DC Converters," IEEE Access, 2022.
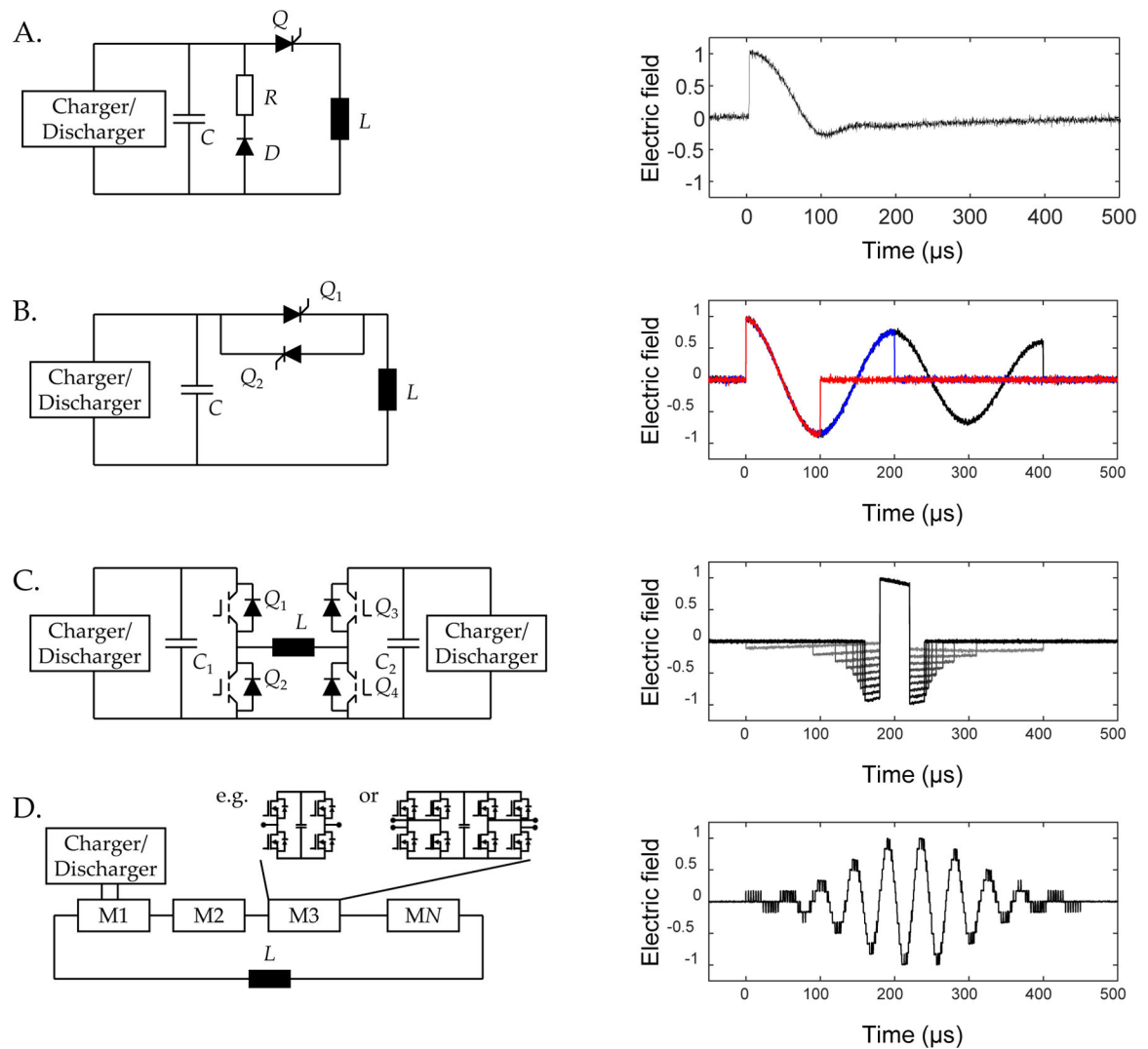
Figure 1.
Circuit topologies (left column) and corresponding typical pulse shapes (right column) of various TMS technologies: A. Monophasic stimulator (typically with thyristors), B. bi- and polyphasic stimulator (existing with thyristors and IGBTs), C. example of a bridge-based TMS device using IGBTs, representing also all other bridge approaches, and D. modular pulse synthesizer. This work implements six four-bridge modules (double H bridge) as shown on the right, which the control can intrinsically operate also as two-bridge modules (H bridge, shown as alternative on the left and compared in Table I). The topology can use chargers and dischargers in several positions. Although every module could have its own charger, a single one in combination with the circuit's charge distribution capabilities is sufficient and can reduce commonmode currents through the parasitic and filter capacitances of the chargers, which are relevant for electromagnetic interference.

A. Cascaded four-bridge modules
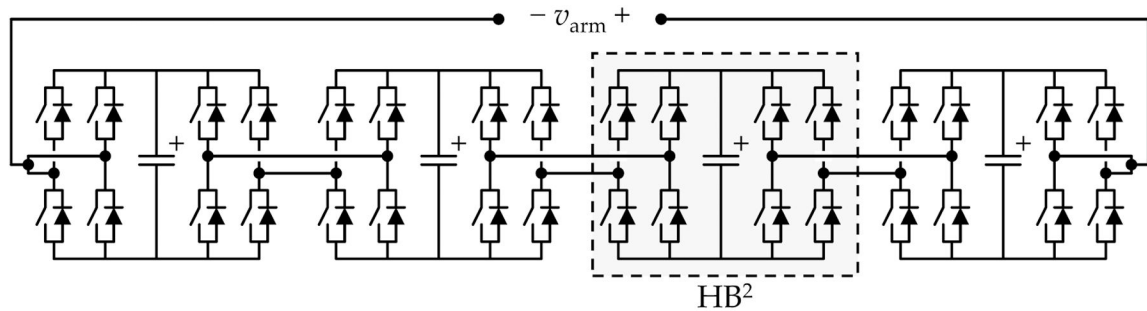
B. Example producing $v_{arm} = 2$
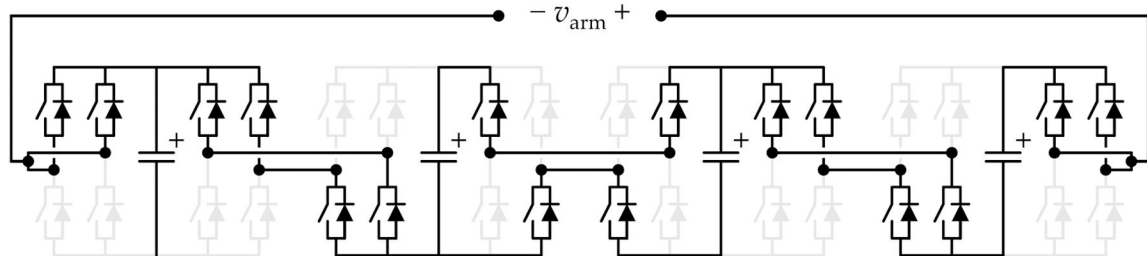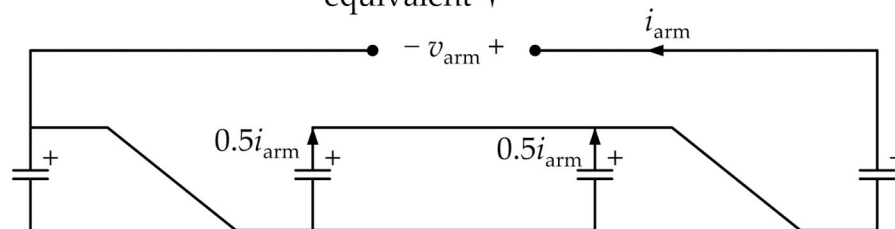
Figure 2.
A. Circuit topology of the power train with here four four-bridge modules. B. Example for a state of the system with two modules including their internal capacitor connected in series and two in parallel to generate two output steps. Alternative two-bridge modules operate similarly, but the parallel mode would have to be replaced by bypass. See Figure 3 for definition of all states.
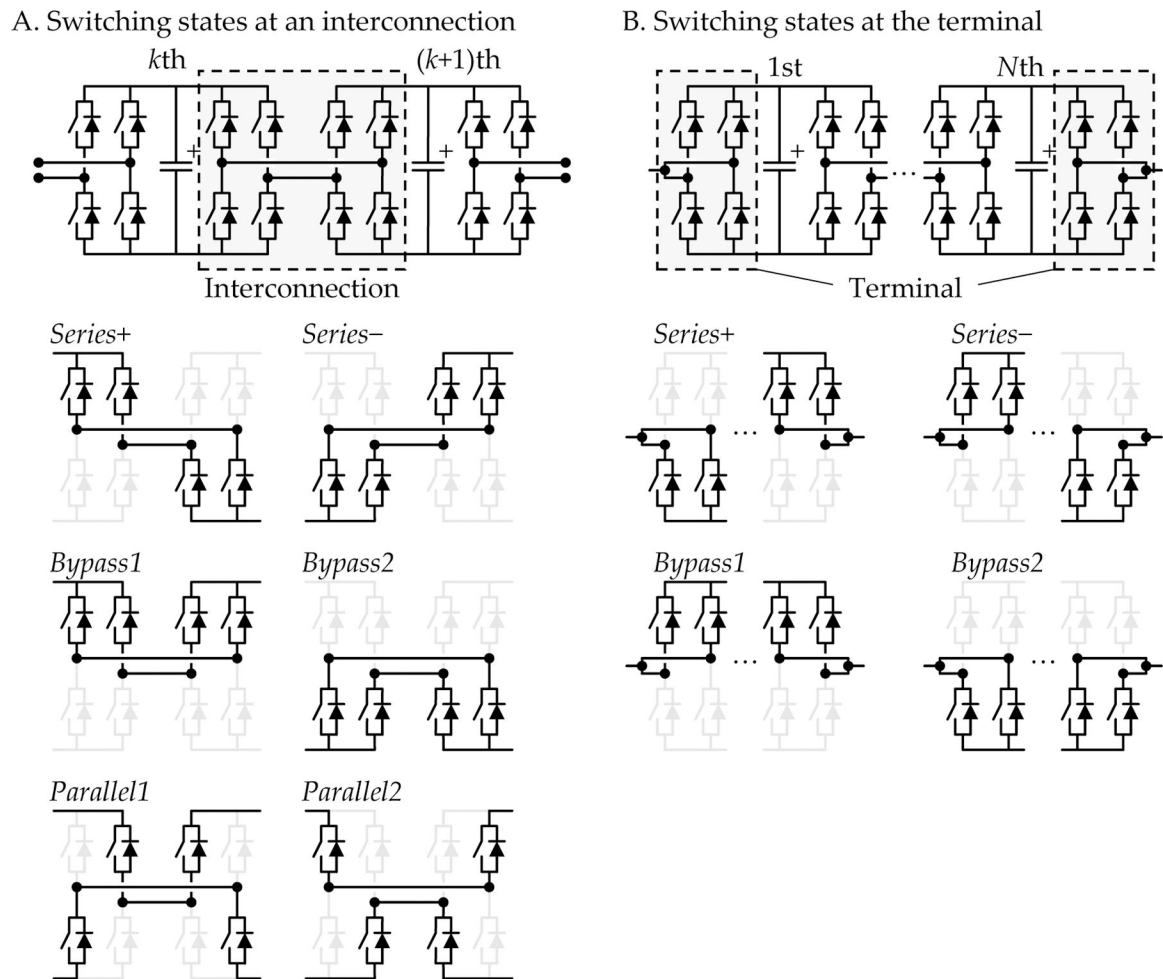
Figure 3.

Switch states of an interconnection A between two modules or B the outmost modules connecting to the coil. The states influence how the capacitors of the modules are electrically connected relative to their neighbors. Two-bridge modules can generate only series and bypass states, four-bridge modules additionally parallel circuit configurations between modules. Series states increase the voltage in positive or negative direction. Parallel modes distribute the current load and balance charge across the capacitors. With fast transistors, the transition from one state to another can occur on the order of 100 ns and several hundred times per millisecond.
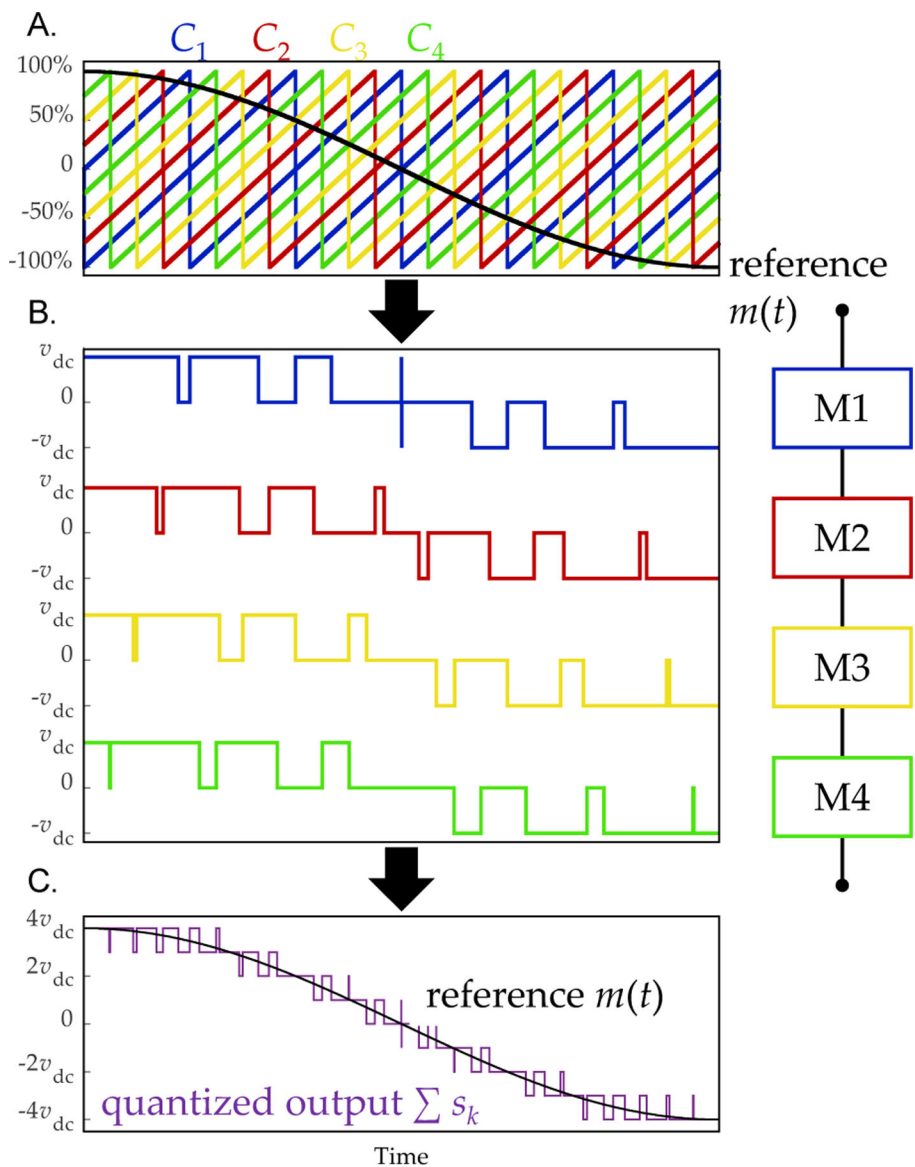
Figure 4.
Principle of phase-shifted carrier modulation (PSC) with here four modules M_k for simplicity and accordingly four carriers C_k. to reproduce the black reference curve $m(t)$. A. Desired reference shape and carrier for comparison, B. module switching states s_k for every module k resulting from the comparison, and C. quantized output following from this modulation.

A. Standard PSC (no compensation) B. Compensate *IR*-drop and dc link
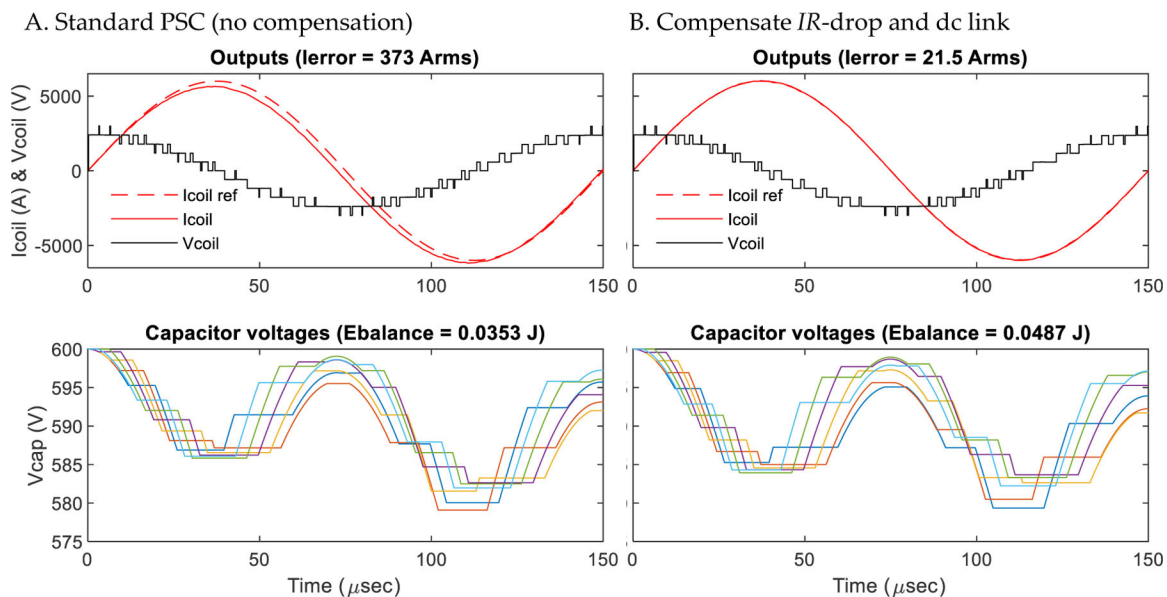
Figure 5.
Simulation results (A) without compensation and (B) with a reference compensating resistive voltage drop and module capacitor voltage variations. The model does not use the parallel mode but only series and bypass to demonstrate how the capacitors drift apart. Parallelization clears such voltage differences.
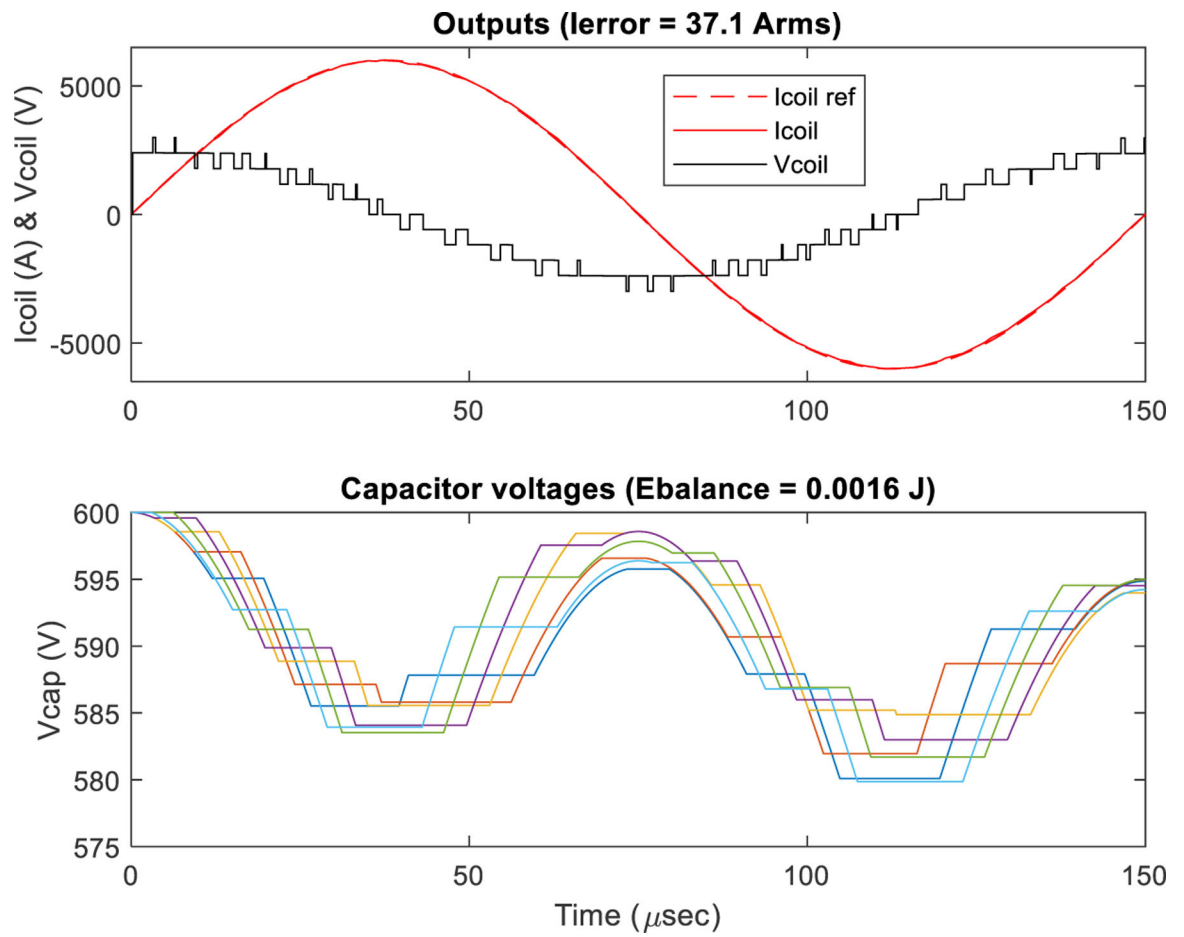
Figure 6.
Simulation results using a reference that compensates the resistive voltage drop, module capacitor voltage variations, and the final module voltage spread.

A. Actual module
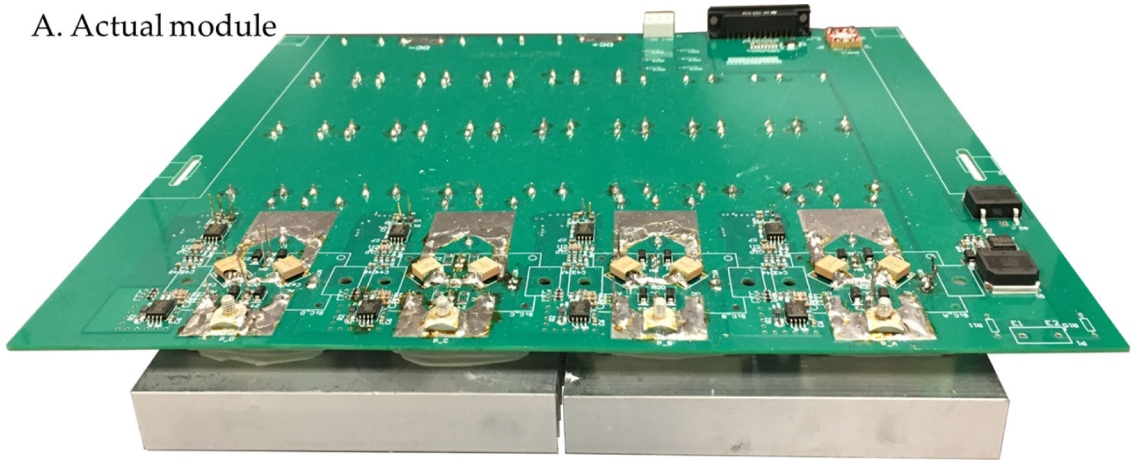
B. Layout design
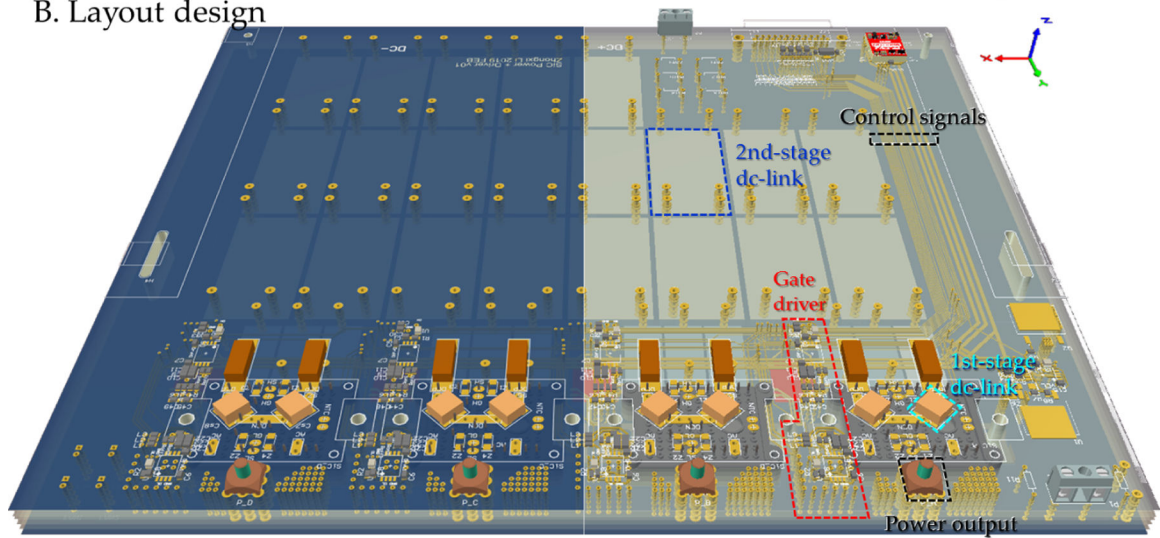
Figure 7.
Circuit board layout (A. actual photo and B. design) with switching cells in the front and capacitance in the back. The transistors are on the bottom side, the driver and first-stage capacitance on the top.
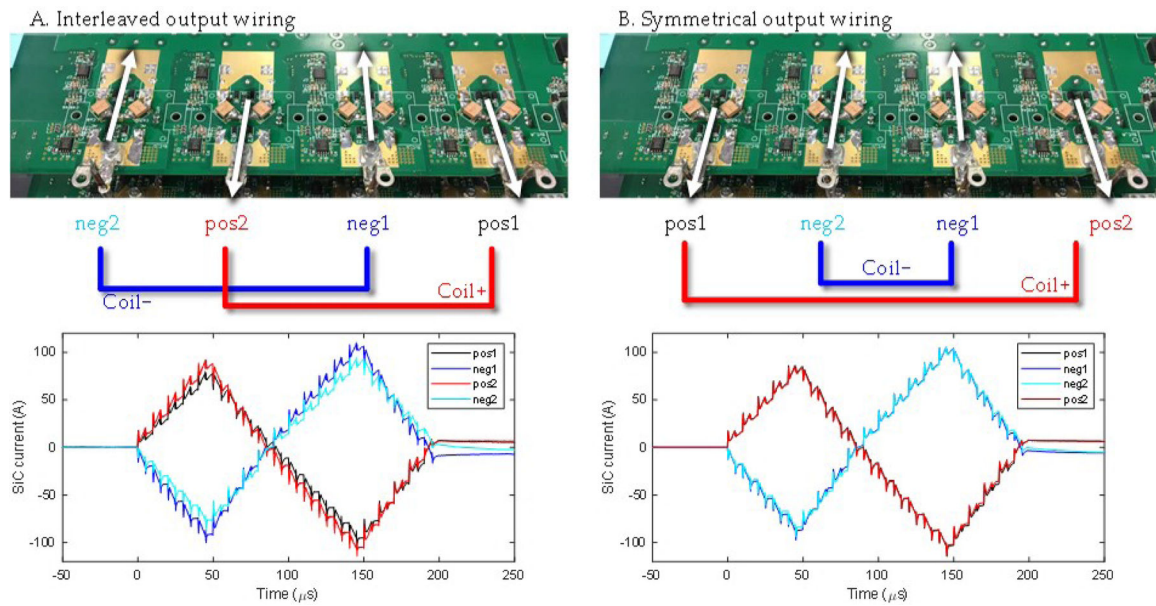
Figure 8.
Two different assignments of four switching cells (discrete pair of high-side and low-side transistor) to two output bridges on one side of a module demonstrating the balance of the current among discrete parallel switching cells. Each switching cell contains discrete transistors (on the back, not visible), gate driver (black ICs between the golden islands), and first-level ceramic capacitance (yellow blocks in V configuration) to absorb the immediate energy demand and/or supply when the parasitic magnetic fields of the commutation current paths is discharged or charged.
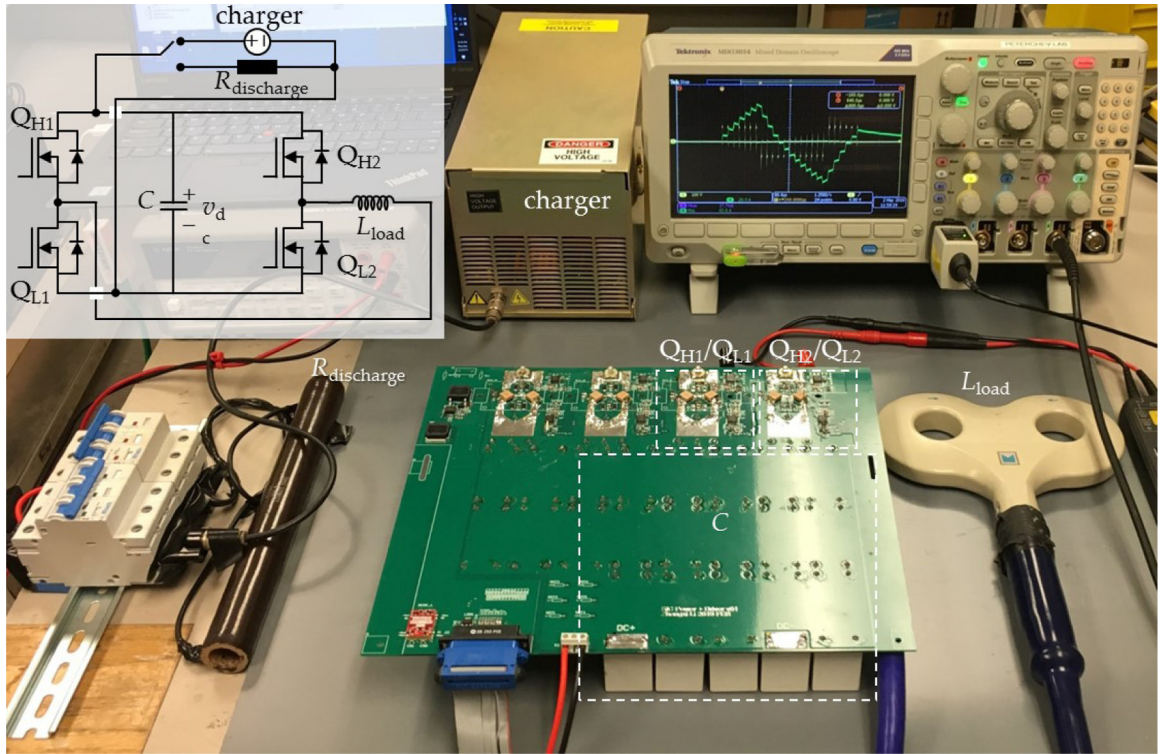
Figure 9.
Double-pulse setup.
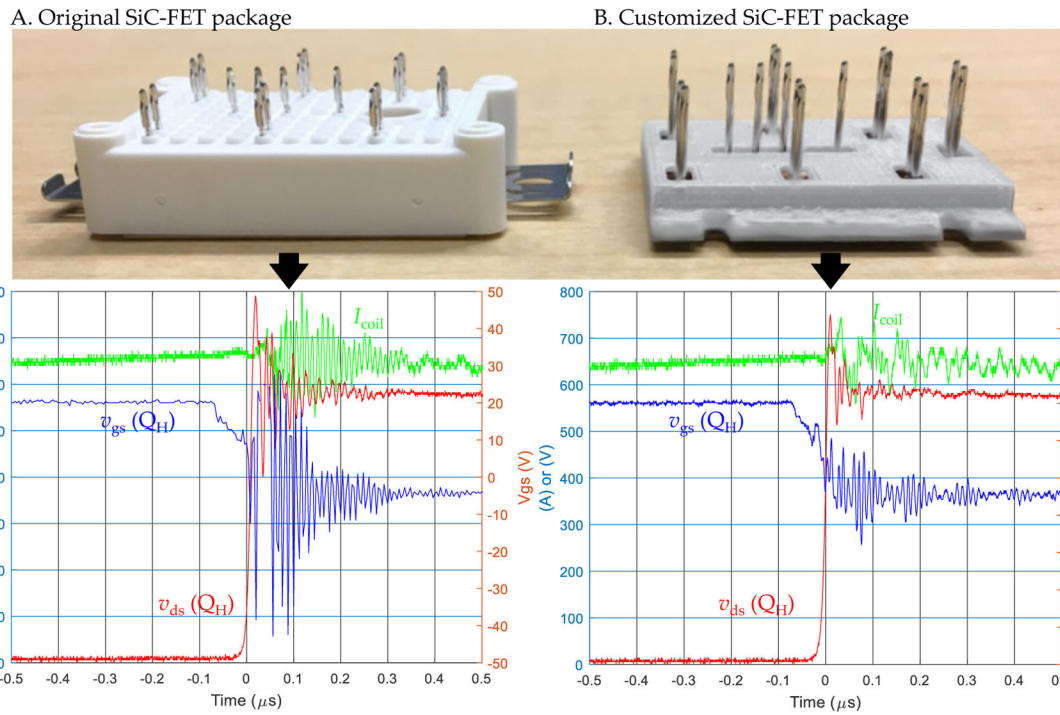
Figure 10.
Example for one of four commutation conditions for A the original FF11 transistor bridge in the optimized layout and B with an optimized package for lower stray inductance. In the measurements, one transistor module is singled out.
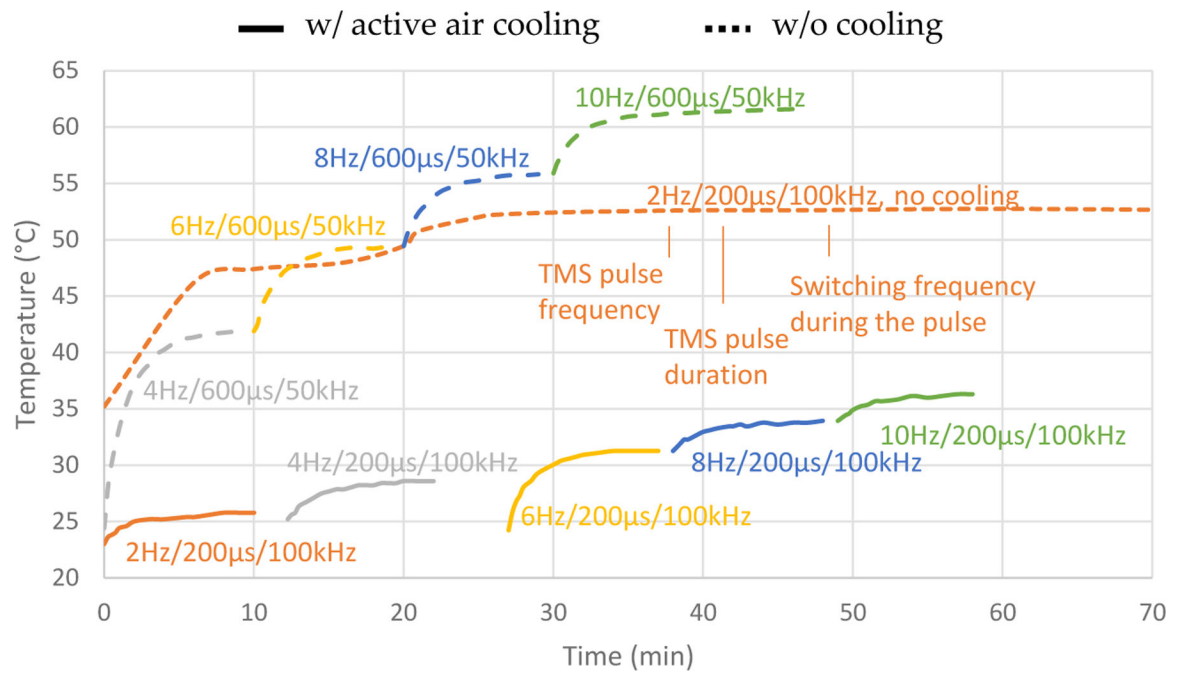
Figure 11.
Temperature development of the SiC transistors under stress testing with sinusoidal current (700 A peak) per discrete transistor (enabling 8,400 A for a module with 12 transistors in our system) and transistor switching rates up to 100 kHz. Dashed lines were performed without any additional cooling in a closed 19" cabinet, solid lines included active air convection, demonstrating a wide margin. The temperature development and the steady-state temperatures show a widely linear relationship with the load as expected. The naming convention is pulse rate (Hz)/pulse duration /switching rate during the pulses.
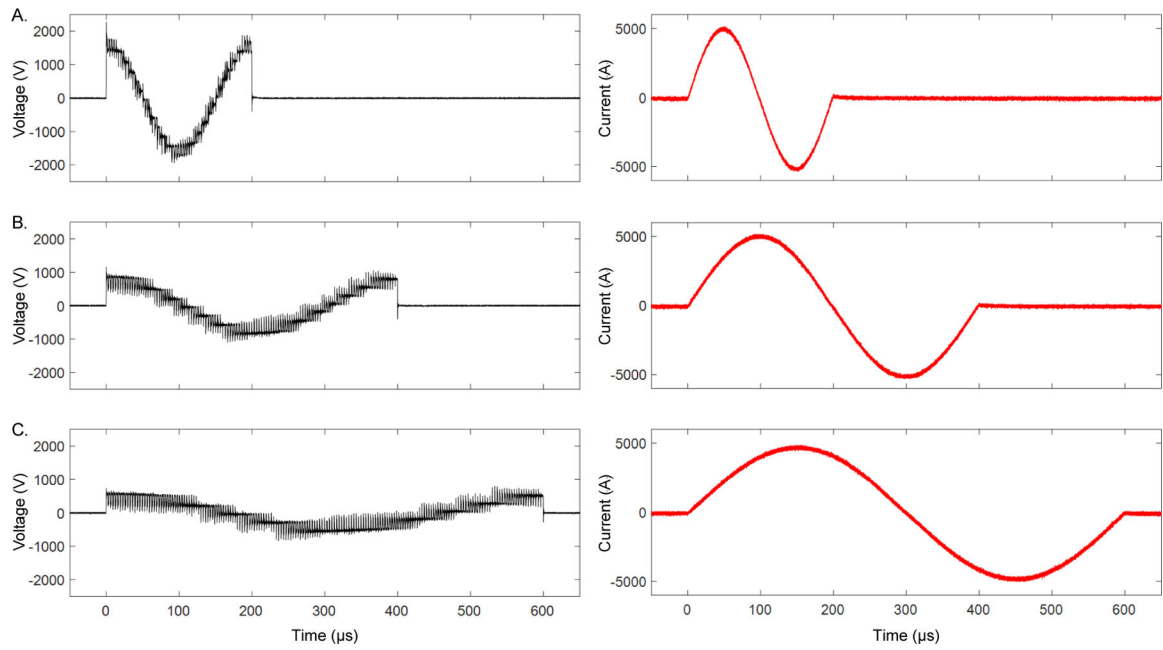
Figure 12.
Recordings of biphasic pulses with cosinusoidal voltage as well as electric field shape and sinusoidal current shape. The pulse shape including its duration is purely software-generated (A 200 μs, B 400 μs, C 600 μs).
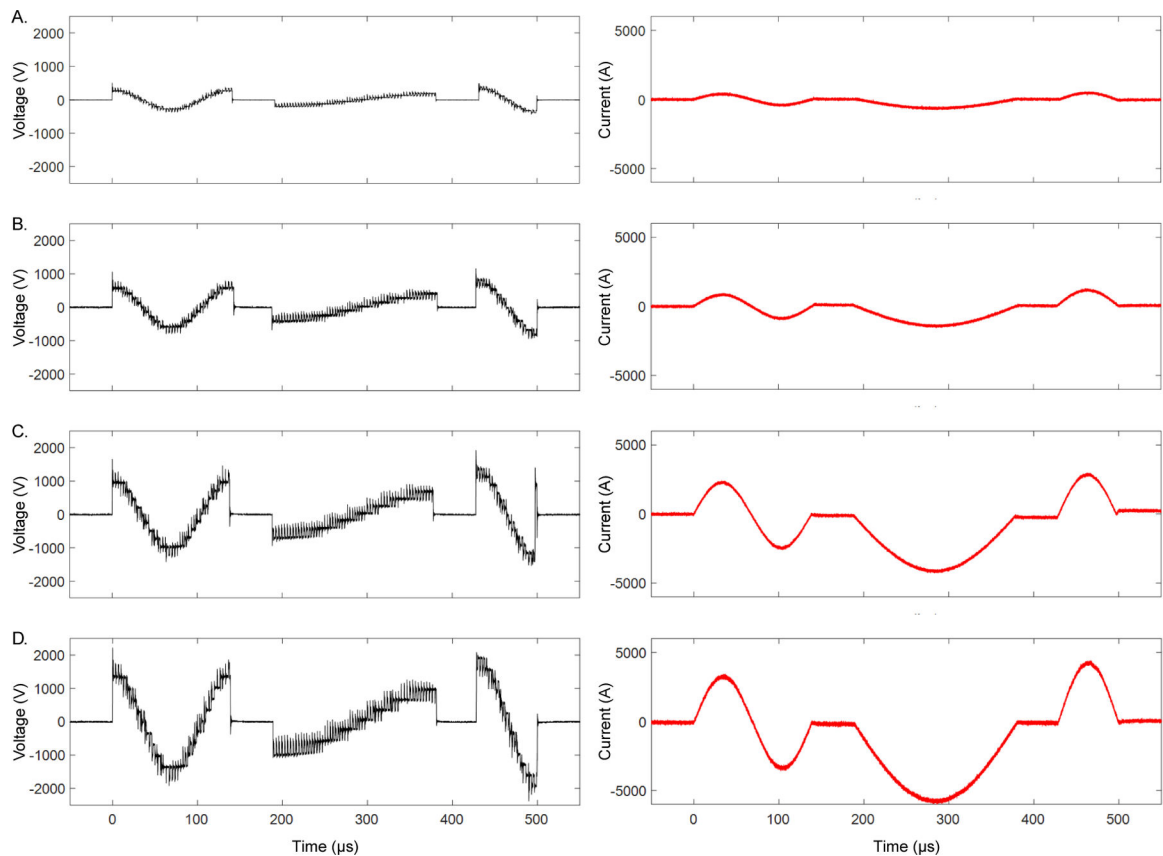
Figure 13.
Recorded pulse train of typical conventional pulses (biphasic and two half-period pulses) with as little as 50 μs between two entirely different pulse shapes. The pulses have different energy content. Still, the device does not need any reconfiguration time or adjustment of charge to change the pulse duration, the pulse amplitude, or change the entire pulse shape. The panels from A to D show the same pulse sequence with increasing pulse amplitude. The recordings demonstrate both ways how the pulse synthesizer can adjust the pulse amplitude: Within a sequence, the circuit uses fewer steps for the lower-amplitude sections and pulses such as the long half-period pulse in the center. From pulse train to pulse train, the circuit increases the amplitude through increasing the module voltage step size.
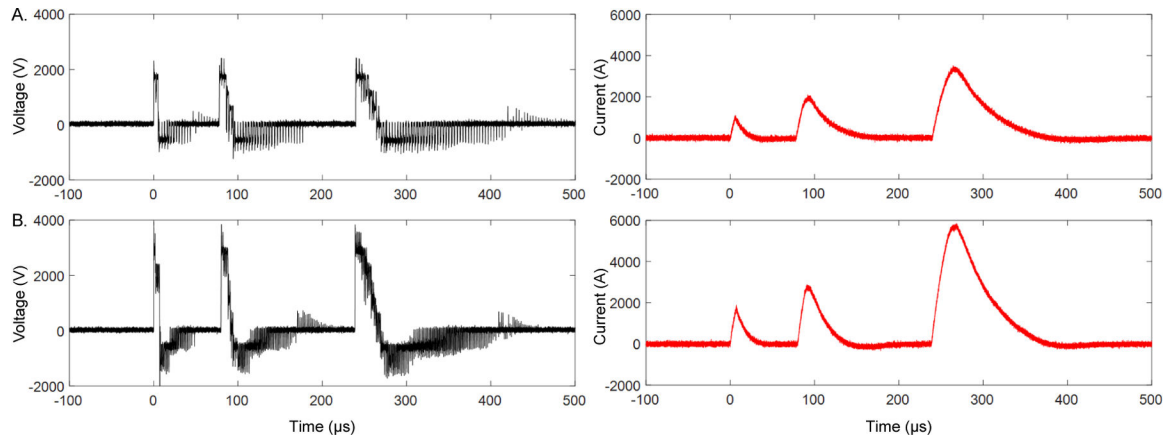
Figure 14.
Sequence of monophasic pulses generated with various pulse durations and in two amplitudes. The approximately exponentially falling phase of the current in the second part of each pulse is generated through resistive damping in conventional monophasic TMS devices associated with the loss of the entire pulse energy. The pulse synthesizer, however, simulates only a resistor to the coil and extracts the energy back to the internal capacitors through proper control so that there is sufficient energy to generate such rapid sequences, which no conventional monophasic device can. Whereas we demonstrated the adjustment of the module voltages to tune the pulse strength in Figure 13, here the lower amplitude of the sequence in Panel A uses less module levels than Panel B to clarify the coarser quantization of this approach.
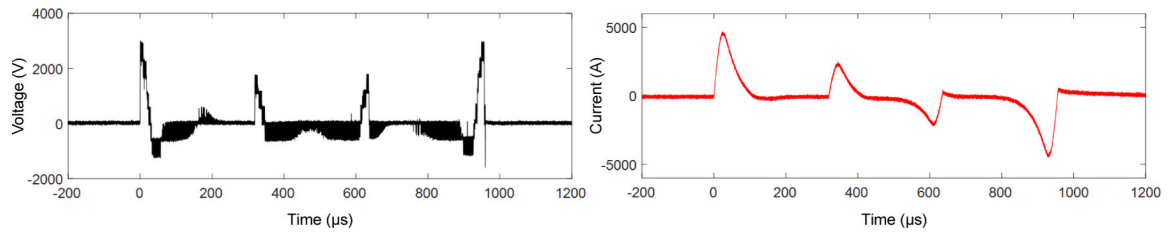
Figure 15.
Burst of various monophasic pulses with different amplitude and time direction. To demonstrate the flexibility and ability to generate practically any pulse shape, the burst does not only change the amplitude but inverses the time direction for the third and fourth pulse so that the voltage is mirrored and the current additionally inverted.
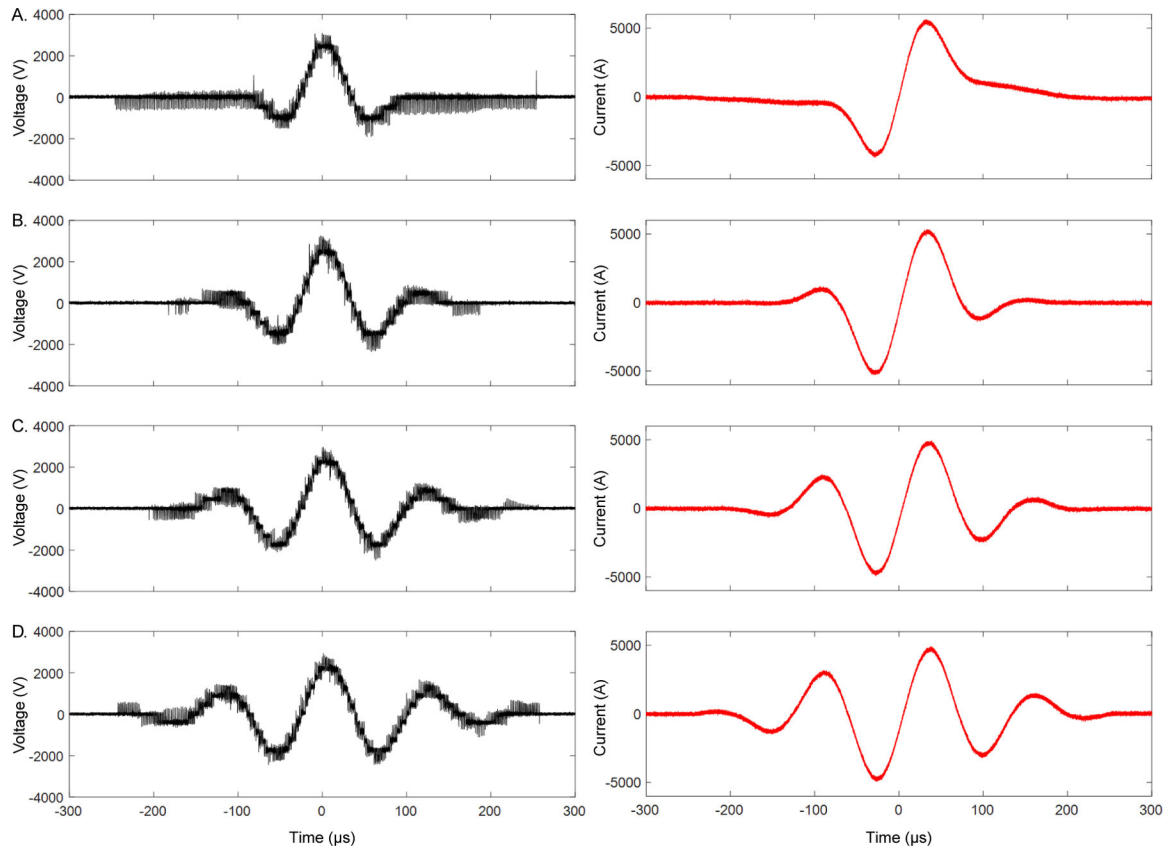
Figure 16.
Polyphasic pulses with sinusoidal current and Gaussian envelope of increasing width from A to D. For very short envelope width, the pulse degenerates into a near-sinusoidal biphasic pulse, which in contrast to conventional biphasic TMS pulses contains smoother edges in the voltage.
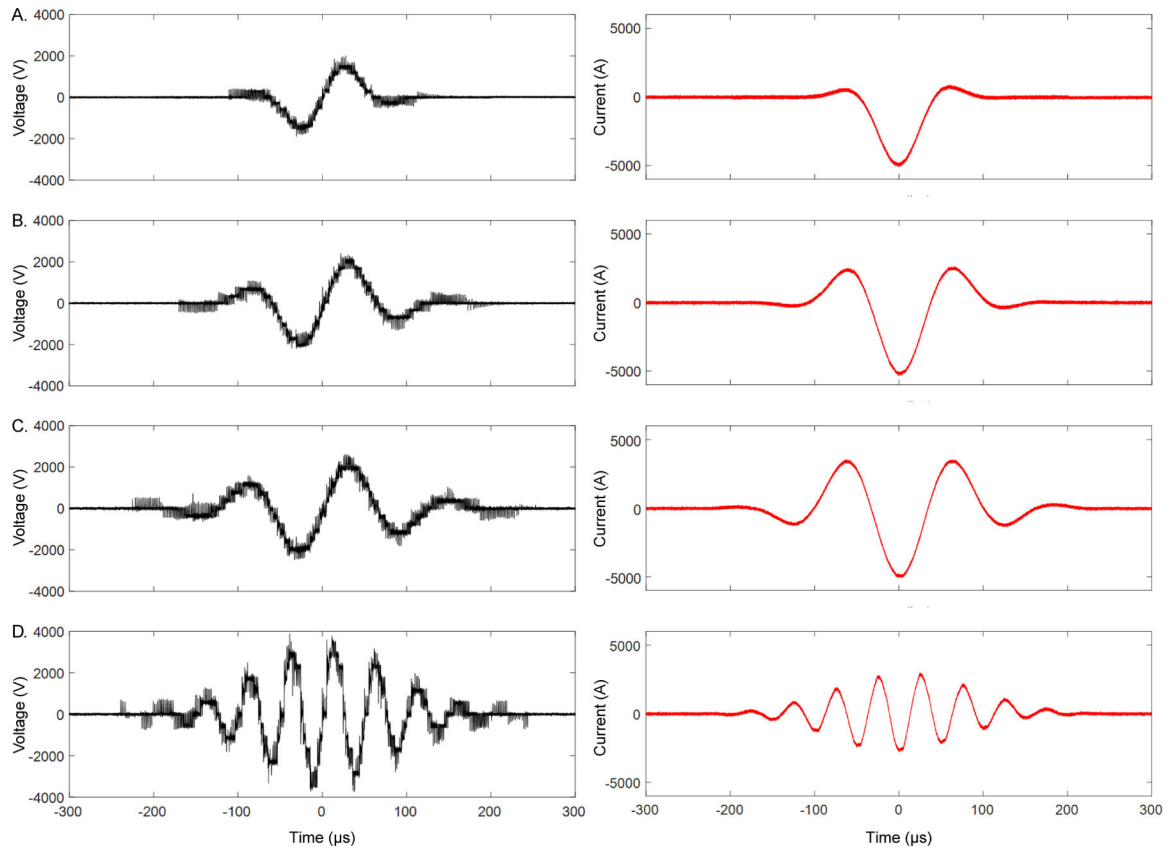
Figure 17.
Polyphasic pulses with cosinusoidal current and Gaussian envelope of increasing width from A to D. For very short envelope width, the pulse degenerates into a near-sinusoidal biphasic pulse, which in contrast to conventional biphasic TMS pulses contains smoother edges in the voltage.
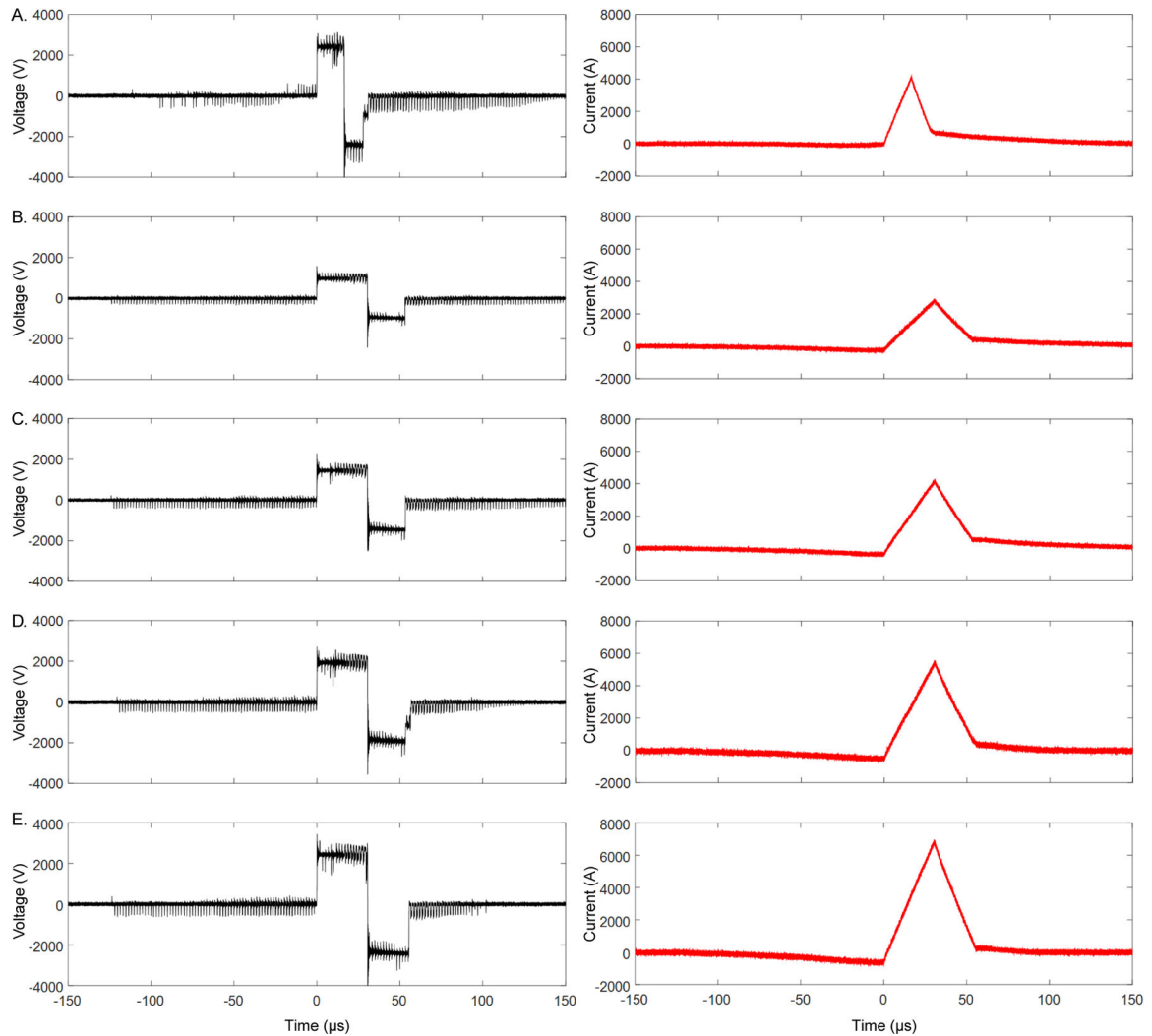
Figure 18.
Pulse shapes optimized for minimum coil heating with different pulse duration (A and B) and various pulse amplitudes for the longer duration (B – E). Before the actual pulse, the device brings the current baseline slowly to a negative offset, from which the current can ramp up with a longer rising edge without reaching large currents. This pre-phase is generated through subtle control of the voltage in the approximately 120 µs introducing the pulse.
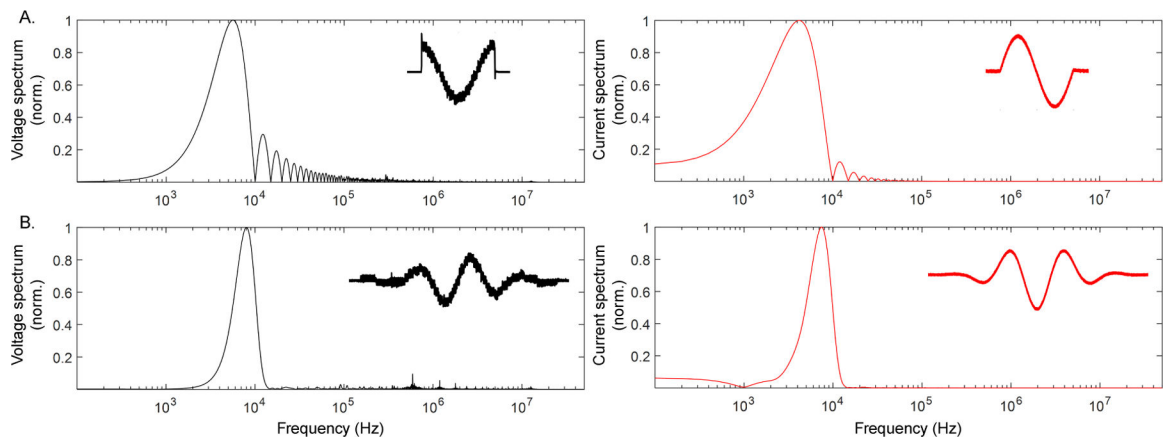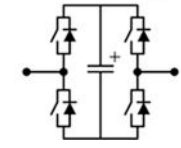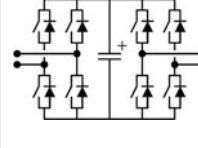
Figure 19.
Unfiltered voltage and current spectra of (A) a biphasic pulse, which may mostly be dominated by an oscillation with one dominant frequency but inherently displays a wide spectrum to its brevity (frequency–time uncertainty principle), and (B) a polyphasic pulse with more periods and Gaussian envelope for a sharper spectrum of the intended pulse. With a careful look, one can see the small residual distortion due to both measurement noise and technical quantization emerging at the right side of the voltage spectrum, in the high-frequency range. The inset in each panel shows the corresponding time course of the voltage or current.

Table I.

Comparison between module alternatives

	Two Bridges	Four Bridges
Topology		
Modulation range	$-1 \quad m \quad 1$ (four-quadrant operation)	
Sensorless-balancing	No	Yes
Discrete switch count	4	8
Switch current rating	i_{arm}	$\frac{1}{2} i_{arm}$
ON-state resistance†	$\frac{1}{2} r_{on}$	r_{on}
Switch conduction loss	$i^2_{arm} r_{on} + 2 \, V_F i_{arm}$	
Capacitor conduction loss	$i^2_{arm} r_{cap} m$	$\frac{1}{2} i^2_{arm} r_{cap} m \sim i^2_{arm} r_{cap} m$

The variable i_{arm} denotes the arm current, r_{on} the effective on resistance of the switches, which can further include also contact resistances, wiring, etc., whereas V_F describes nonresistive forward voltages; r_{cap} represents the equivalent resistance of the capacitors.

Table II.

Key components of the power stage

Component	Key parameter or quantity	Part number	Manufacturer
Module power transistors	24×	FF11MR12W1M1	Infineon
First-stage module capacitance	12 μF	B58031U9254M062	EPCOS/TDK
Second-stage module capacitance	194 μF	C4AQQBU4270A1XJ	Kemet
Third-stage module capacitance	1.8 mF	C4AQQBW5300A3MJ	Kemet
Gas discharge tubes	1 kV, 130 A	CG21000L	Littelfuse
Gate driver	6 A	1EDI60H12AH	Infineon
Gate supply	+19 V/–5 V	MGJ1D121905MPC-R7	Murata
CM gate supply filter	4 A	BU05MC08T	Taiyo Yuden
Gate energy storage	170 μF	TMK212AB7475KG-T	Taiyo Yuden
Gate supply limiter positive	20 V	SMBJ20A	Littelfuse
Gate supply limiter negative	–6 V	SMBJ6.0A	Littelfuse
Module discharge relay	7 kV, 2 A	DBT71210U	Cynergy3 Components
Module discharge resistors	700 V	AP101 470R J	Ohmite Manufacturing
Module discharge relay drive	20 V, 1.2 A	IRLML2402TRPBF	Infineon
Logic supply	12 V, 2.5 A	RAC30–12SA	Recom Power
Bus signal isolators	100 Mbps, 8 kV pk isolation	ISO7841FDWW	Texas Instruments
Central bus drivers	16 ns slope time	UCC27712QDQ1	Texas Instruments
Power supply	1000 W	00493189 102A	Lambda Power
Fast module controller	CPLD	10M02SCE144I7G	Altera/Intel
Module monitoring controller	Mixed signal processor	MSP432P401RIPZR	Texas Instruments
Central controller	System on chip	sbRIO 9627 Zynq 7000	National Instruments/AMD/Xilinx